Modulation of global transcriptional regulatory networks as a strategy for increasing kanamycin resistance of EF-G mutants

Aalap Mogre and Aswin Sai Narain Seshasayee

National Centre for Biological Sciences, Tata Institute of Fundamental Research, GKVK, Bellary Road, Bangalore, Karnataka 560065, India

Corresponding Authors:

Aswin Sai Narain Seshasayee

National Centre for Biological Sciences, Tata Institute of Fundamental Research, GKVK, Bellary Road, Bangalore, Karnataka 560065, India

Email id: aswin@ncbs.res.in

Aalap Mogre

National Centre for Biological Sciences, Tata Institute of Fundamental Research, GKVK, Bellary Road, Bangalore, Karnataka 560065, India

Email id: aalapbm@ncbs.res.in

Abstract

Evolve and resequence experiments have provided us a tool to understand bacterial adaptation to antibiotics by the gain of genomic mutations. In our previous work, we used short term evolution to isolate mutants resistant to the ribosome targeting antibiotic kanamycin. We had reported the gain of resistance to kanamycin via multiple different point mutations in the translation elongation factor G (EF-G). Furthermore, we had shown that the resistance of EF-G mutants could be increased by second site mutations in the genes *rpoD* / *cpxA* / *topA* / *cyaA*. In this work we expand on our understanding of these second site mutations. Using genetic tools we asked how mutations in the cell envelope stress sensor kinase ($CpxA^{F218Y}$) and adenylate cyclase ($CyaA^{N600Y}$) could alter their activities to result in resistance. We found that the mutation in *cpxA* most likely results in an active Cpx stress response. Further evolution of an EF-G mutant in a higher concentration of kanamycin than what was used in our previous experiments identified the *cpxA* locus as a primary target for a significant increase in resistance. The mutation in *cyaA* results in a loss of catalytic activity and probably results in resistance via altered CRP function. Despite a reduction in cAMP levels, the $CyaA^{N600Y}$ mutant has a transcriptome indicative of increased CRP activity, pointing to an unknown non-catalytic role for CyaA in gene expression. From the transcriptomes of double and single mutants we describe the epistasis between EF-G mutant and these second site mutations. We show that the large scale transcriptomic changes in the topoisomerase I ($FusA^{A608E}$-$TopA^{S180L}$) mutant likely result in supercoiling changes in the cell. Finally, genes with known roles in aminoglycoside resistance were present among the mis-regulated genes in the mutants.

Introduction

The efficacy of antibiotics, once heralded as miracle drugs, is now under threat because of the emergence of resistance (Davies, 1996; Levy & Marshall, 2004). One way in which bacteria become resistant to antibiotics is by gaining genomic mutations. These genomic mutations tend to accumulate mostly in the target of the antibiotic, and more often than not result in a fitness defect because these target genes tend to be essential or important for cell growth (Lenski, 1998; Andersson & Levin, 1999; Björkman & Andersson, 2000; Andersson, 2006; Andersson & Hughes, 2010). Resistance can also evolve via mutations in non-target genes (Kern et al., 2000), and studying such mutations will yield insight into the mechanism of action of the antibiotic inside the bacterial cell.

Aminoglycosides, a group of ribosome targeting antibiotics (Becker & Cooper, 2013), have a target that is difficult to modify mutationally. This difficulty arises, especially in fast growing organisms like *E. coli*, because of the presence of multiple copies of the gene encoding the target of aminoglycosides, i.e. the 16S rRNA. On short timescales, it is not possible to mutate all copies of the target gene, seven of which are present in *E. coli* for instance, to achieve resistance (Kotra, Haddad & Mobashery, 2000).

In our previous work, we evolved *E. coli* in different sublethal levels of a model aminoglycoside kanamycin (Mogre et al., 2014). We obtained multiple kanamycin resistant mutants of the translation elongation factor EF-G (FusA). At the lower 4-kan (4 μg/ml; 25% lethal concentration kanamycin), we found a single point mutation in EF-G ($FusA^{P610T}$), whereas at the higher 8-kan (50% lethal concentration kanamycin), we found two different point mutations in EF-G ($FusA^{A608E}$ and $FusA^{P610L}$). The $FusA^{P610T}$ allele dominated evolved populations for five transfers (rounds of subculture) in 4-kan; whereas in 8-kan, the $FusA^{A608E}$ allele appeared in the first round of growth, followed by the $FusA^{P610L}$ allele in the next transfer. Among the three EF-G mutants, the $FusA^{P610L}$ allele had the best growth in 8-kan. Interestingly the $FusA^{A608E}$ allele had also accumulated second site mutations in four genes, viz., *rpoD*, *cpxA*, *topA* and *cyaA*, in four different isolates. Apart from our work, evolution experiments in aminoglycosides done by Lazar et al., have revealed resistance conferring mutations in *fusA*, *rpoD*, *cpxA* and *crp*, but not in *cyaA* and *topA* (Lázár et al., 2013).

EF-G is a translation factor and a part of this protein, specifically the tip of domain IV, interacts with the decoding centre, the binding site of aminoglycosides (Feldman et al., 2010). Thus, whereas the contribution of EF-G - a factor associated with the binding site of the antibiotic - to resistance is easier to understand, the mechansims by which these second site mutations confer resistance are not immediately apparent. Interestingly, all of the above second site mutations could affect transcription. More specifically, RpoD is the major sigma factor responsible for much of transcription in exponentially-growing *E. coli* (Feklístov et al., 2014). CpxA is an envelope stress sensor kinase, which by phosphorylating its response regulator CpxR, activates the expression of genes that tackle membrane stress (Hunke, Keller & Müller, 2012). Activation of the Cpx response upon antibiotic exposure was thought to result in increased oxidative stress and consequently cell death (Kohanski et al., 2008).

However, more recent work has shown that Cpx activation confers resistance and not sensitivity to certain antibiotics (Mahoney & Silhavy, 2013; Manoil, 2013). Topoisomerase I (TopA) relaxes negatively supercoiled DNA, and can thereby affect the transcription of many genes (Travers & Muskhelishvili, 2005). Adenylate cyclase (CyaA) produces cAMP (cyclic adenosine monophosphate), a cellular second messenger, that can influence the expression of a large number of genes via the global regulator CRP (cAMP Receptor Protein) (Zheng et al., 2004). Furthermore, Girgis et al., were able to show that disruptions of *cyaA* and *crp* were beneficial to growth in aminoglycosides (Girgis, Hottes & Tavazoie, 2009).

To understand the contribution of these second site mutations to kanamycin resistance, we first generated their single mutant versions. We found that the second site mutations by themselves provide only a marginal increase, if any, in growth in kanamycin. These second site mutations however allow better growth in kanamycin in either the FusA^{P610T} or the FusA^{A608E} background. By comparing these second site mutants with their corresponding whole gene deletions, we attempted to clarify their roles in kanamycin resistance. Further, using RNA-seq, we found a non-additive effect between the mutation in EF-G and that in the second-site on gene expression. By comparing our transcriptome data with previously published datasets, we provide tentative evidence for elevated negative supercoiling in the chromosome of the FusA^{A608E}-TopA^{S180L} mutant. Lastly, we were able to see sets of genes with known roles in aminoglycoside resistance among those mis-regulated in these mutants. This reinforces the idea that mutating promiscuous regulators of transcription might be an effective early strategy for adaptation to stress.

Materials & Methods

Strain construction

All strains used had the non-pathogenic *E. coli* K12 MG1655 background. RpoD^{L261Q}, CpxA^{F218Y} and CyaA^{N600Y} mutants were constructed from their respective FusA^{A608E}-RpoD^{L261Q} / CpxA^{F218Y} / CyaA^{N600Y} double mutants by replacing the FusA^{A608E} allele with the wildtype *fusA* allele linked to a kanamycin resistance cassette. This was done by P1 phage transduction according to the Court lab protocol (Thomason, Costantino & Court, 2007). Selection with a higher concentration of kanamycin (70-80 μg/ml) ensured that only transductants with the wildtype *fusA* linked to the kanamycin resistance cassette were selected, and that the non-transduced recipient double mutants were not. Background growth of the non-transduced double mutants was a common problem, however only the best growing colonies were picked since these would contain the kanamycin resistance cassette. All transductants were verified by PCR to ensure the presence of the kanamycin cassette. The kanamycin resistance cassette was flanked by FRT sites and thus was flipped out using the site specific recombinase Flp provided by the plasmid pCP20. Finally the temperature sensitive plasmid pCP20 was cured from these cells by growing them at 42 ^{0}C. The wildtype strain containing the kanamycin cassette near *fusA* was also treated similarly to generate a strain containing the FRT site near *fusA* (WTfrt) and was used as the reference strain. The mutations in *fusA*, *rpoD*, *cpxA*, *topA* and *cyaA* were checked by Sanger sequencing.

Knockout strains Δ*cyaA*::*kan*^{R}, Δ*crp*::*kan*^{R} were earlier generated in the lab, whereas Δ*cpxA*::*kan*^{R} and Δ*cpxR*::*kan*^{R} were obtained from Coli Genetic Stock Center (CGSC). These knockouts were transferred into the wildtype used in this study, FusA^{P610T} and FusA^{A608E} strains by phage transduction. The process outlined above was used to get rid of the kanamycin resistance cassette after transferring the gene knockouts to the relevant strains including the wildtype used in this study.

Growth curves and Minimum Inhibitory Concentration (MIC) determination

Growth curves were performed in Luria-Bertani broth (LB) in either flasks or 96-well plates. For the purpose of sample collection and RNA extraction growth curves were performed in flasks at 37 ^{0}C, 200 rpm with optical density readings measured at 600 nm using a Metertech SP-8001 Spectrophotometer. For strain comparisons, growth curves were performed in 96-well plates. These growth curves were performed using the Tecan Infinite F200pro plate reader. The machine incubated the plate at 37 ^{0}C and carried out shaking at 198 rpm with optical density readings measured at 600 nm every 15 minutes.

MICs were measured as previously described, using a modification of the broth dilution technique (Mogre et al., 2014).

Cyclic adenosine monophosphate (cAMP) estimation

Estimation of intracellular cAMP levels was carried out using the cyclic AMP Select EIA kit (501040, Cayman Chemical). Cells growing exponentially (~1.5 hours in LB) and in the stationary phase (~12-15 hours in LB) were harvested by centrifugation at 13,000 g for 1 minute. Cells were immediately transferred onto ice to prevent breakdown of cAMP by phosphodiesterases. Cell pellets were washed once with TBST (20 mM Tris, 150 mM NaCl, 0.05% Tween 20, pH 7.5) before being resuspended in 0.05 N HCl. Cells were then boiled for 5 minutes to extract cAMP. Cells were then spun down at maximum speed and the supernatant containing cAMP was collected. Estimations of cAMP were carried out according to the kit's instructions with the exception that the provided cAMP standard was diluted in 0.05 N HCl to generate the standard curve, since HCl was used for the extraction process.

Evolution in kanamycin

The MIC of kanamycin of the $FusA^{P610T}$ mutant was around 60 μg/ml. 25% of this concentration, i.e. 15 μg/ml, was selected for evolving $FusA^{P610T}$ towards higher resistance. Evolution experiments were carried out by batch transfers in LB with and without kanamycin. Two overnight grown replicate populations of *E. coli* were diluted 1:100 in 100 ml LB containing 15 μg/ml kanamycin and 100 ml plain LB as control. Thus two populations evolving in 15 μg/ml kanamycin and two control populations evolving in plain LB were incubated at 37 ^{0}C, 200 rpm for 24 hours before the next transfer. Each evolving population was transferred by 1:100 dilution into fresh medium. The concentration of kanamycin was not changed during the course of the evolution experiment. MICs of all populations were followed at the end of each transfer.

Genomic DNA was extracted from both control and experimental populations using the GenElute Bacterial Genomic DNA Kit (NA2120, Sigma-Aldrich). Integrity of the extracted gDNA was checked on agarose gel, and quality and concentration were checked using NanoDrop UV-Vis Spectrophotometer (Thermo Scientific). Library preparation for deep sequencing was carried out using the Truseq Nano DNA Library Preparation Kit (FC-121-4001, Illumina).

Paired end sequencing was carried out using the Illumina HiSeq sequencer (2 x 100 Cycles) at the Next Generation Genomics Facility, Centre for Cellular and Molecular Platforms (C-CAMP). FASTX quality filtered reads were trimmed using CUTADAPT version 1.9.dev1 (Martin, 2011), to remove adapter sequences. Error tolerance in identifying adapters was set to 20% and trimmed reads with less than 30 bases were discarded. These trimmed reads, were then mapped to the *E. coli* K12 MG1655 reference genome (NC_000913.3) using BWA mem version 0.7.5a-r405 (Li & Durbin, 2010); paired files were input together at this step. SAMTOOLS version 1.3 (Li et al., 2009) was then used to generate the pileup file from the sam files generated by BWA. Finally, the list of single nucleotide polymorphisms (SNPs) and indels was compiled from the pileup file using VARSCAN version 2.3.8 (Koboldt et al., 2012).

RNA extraction, sequencing and analysis

For RNA extraction, cells were grown in LB and harvested at the point of maximal growth rate (Fig. S1) after the addition of stop solution to stabilise cellular RNA and stop transcription. Two biological replicates were harvested for each strain including the reference strain WTfrt. RNA was extracted using the hot phenol-chloroform method. DNase treated RNA was depleted of ribosomal RNA using the Ambion Microbe Express Kit (AM1905). RNA was checked for quality using Bioanalyzer (Agilent). Checked RNA was used for library preparation and sequencing. RNA quality checks, library preparation and sequencing were carried out at Genotypic (India). Briefly, 100 ng of qubit quantified RNA was used for library preparation using the NEXTflex Rapid Directional RNA-Seq kit (5138-08 Bioo Scientific). The library was quantified using qubit and its quality was checked using Agilent Bioanalyzer before proceeding for sequencing on the Illumina NextSeq 500 sequencer.

FASTX filtered reads were trimmed using CUTADAPT and aligned to the *E. coli* reference genome (NC_000913.3) using BWA. SNP and indel calling was done to ensure that the correct mutations were present in the relevant samples (Fig. S2). The number of reads mapping to each gene was obtained using custom Python scripts. Correlation of raw read counts between replicates were high (>0.9, Fig. S3). Even across different strains, the strength of correlation was high (> 0.8, Fig. S3). We also checked that genes within operons were similarly expressed (Fig. S4).

Subsequently the R (R Core Team, 2016) package EdgeR (Robinson, McCarthy & Smyth, 2010) was used to call differentially expressed genes using a P value cutoff of 0.001 (using the Benjamini Hochberg method to control the false discovery rate in multiple testing).

Gene ontology analysis was carried out using the R package topGO (Alexa & Rahnenfuhrer, 2010). *E. coli* gene annotations were obtained from Ecocyc (Karp et al., 2014) and gene ontology terms were obtained from the Gene Ontology Consortium (Gene Ontology Consortium, 2015). In topGO, the Fisher test was used to assess significance of enriched gene sets and terms with P values < 0.01 were considered significant.

Results and Discussion

Second site mutations increase kanamycin resistance of EF-G mutants.

In our previous work we had found that four 'second-site' mutations, namely RpoD^{L261Q}, CpxA^{F218Y}, CyaA^{N600Y} and TopA^{S180L}, appeared on a FusA^{A608E} background in 8-kan. The double mutants had marginally greater resistance to kanamycin, as measured by their MICs, than the single FusA$^{P610T/A608E}$ mutants and was statistically significant in the case of the FusA^{A608E} mutant, but not the FusA^{P610T} mutant (Fig. 1A). However, the double mutants grew to a higher cell density in 8-kan, thus pointing to their selective advantage over the single mutant in kanamycin (Fig. 1B).

We replaced the FusA^{A608E} mutation in all the double mutants with the FusA^{P610T} mutation that had evolved in the wildtype background in 4-kan. The FusA^{P610T} mutation showed sub-optimal growth under conditions in which FusA^{A608E} and its second-site mutants emerged (8-kan, Fig. 1B). These FusA^{P610T} double mutants grew to a higher cell density than the FusA^{P610T} single mutant alone in 8-kan (Fig. S5, control growth curves in 0-kan in Fig. S6). Thus, the selective advantage conferred by these second site mutations was similar between the two primary FusA mutants.

We constructed single mutant versions of RpoD^{L261Q}, CpxA^{F218Y} and CyaA^{N600Y} from their respective double mutants by replacing the mutant FusA^{A608E} allele with the wildtype allele (see Materials & Methods). For reasons not understood, we were unable to construct the TopA^{S180L} single mutant. We saw that the resistance of the double mutants decreased to almost wildtype levels in these single second-site mutants (Fig. 1C). This is seen more clearly in the growth curves of these single mutants in 8-kan (Fig. 1D). These single mutants, however, fared better than the wildtype at a very low concentration of kanamycin (Fig. 1E).

From the order of occurrence of mutations in our evolution experiments, and the inability of single mutants of *cpxA*, *cyaA* and *rpoD* to grow well in kanamycin, it is reasonable to suggest that the mutation in EF-G potentiates the second site mutations, which further increase its resistance. Lazar et al., from their large scale evolution experiments in a range of aminoglycosides have provided us with a valuable list of resistance conferring mutations. It would be interesting to know the order of occurrence of their mutations, and to know which mutations coexist with each other.

Mutation in the extra-cytoplasmic stress sensor CpxA results in resistance via hyper-activation of the Cpx stress response

The Cpx stress response is mediated by the CpxA sensor kinase and its cognate response regulator CpxR (~58 targets in RegulonDB). This versatile two-component system responds to various kinds of stress signals, especially those associated with membrane stress (Pogliano et al., 1997; Raivio & Silhavy, 1997; Hunke, Keller & Müller, 2012; Vogt & Raivio, 2012). Aminoglycosides cause the accumulation of misfolded proteins in the cell membrane and periplasmic space (Bryan & Kwan, 1983; Davis, 1987; Kohanski et al., 2008). The Cpx system

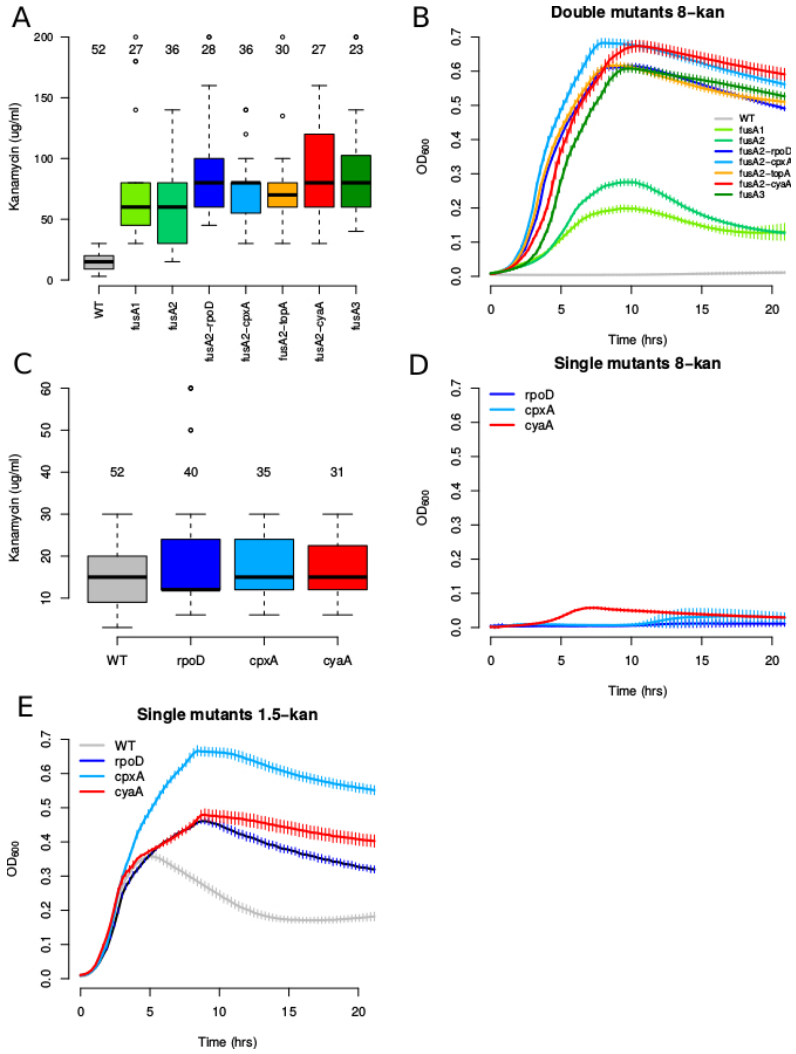

Figure 1: ***Kanamycin resistance of mutants.*** *(A) Boxplots showing distributions of Minimal Inhibitory Concentrations (MICs) of kanamycin of the wildtype and various mutants. Wildtype is represeted as WT and mutants are represented by gene names for brevity. The three fusA alleles are represented by numbers, i.e fusA1, fusA2 and fusA3, and stand respectively for FusA^{P610T}, FusA^{A608E} and FusA^{P610L}. The number of replicates is mentioned over each boxplot. All mutants are significantly more resistant than the wildtype (Welch two sample t-test, P value < 10^{-7}). Although the medians of the FusA^{A608E}-RpoD^{L261Q} / CpxA^{F218Y} / TopA^{S180L} / CyaA^{N600Y} double mutants tend to be higher than that of the FusA^{P610T} mutants, this difference is not statistically significant (P value > 0.09). The difference between the medians of the double mutants and the FusA^{A608E} mutant are statistically significant (P value < 0.02), except in the case of the FusA^{A608E}-TopA^{S180L} mutant (P value 0.061) (B) Growth of mutants in 8-kan. Although MICs of the FusA^{A608E}-RpoD^{L261Q} / CpxA^{F218Y} / TopA^{S180L} / CyaA^{N600Y} double mutants are not significantly higher, they grow better than the FusA^{P610T} or FusA^{A608E} mutants in 8 µg/ml kanamycin. (C) Boxplots showing distributions of MICs of the wildtype, and second site RpoD^{L261Q}, CpxA^{F218Y} and CyaA^{N600Y} single mutants. Their MIC levels are similar to that of the wildtype. (D) Growth of the RpoD^{L261Q}, CpxA^{F218Y} and CyaA^{N600Y} single mutants mutants in 8-kan. These mutants don't grow well in 8-kan. (E) Growth of the RpoD^{L261Q}, CpxA^{F218Y} and CyaA^{N600Y} mutants in 1.5-kan. These mutants grow better than the wildtype at this concentration of kanamycin.*

responds to this stress (Kohanski et al., 2008). It was thought that the crosstalk of the Cpx response with the redox reactive Arc two-component system results in oxidative stress that kills cells (Kohanski et al., 2008). However, more recent genetic experiments have revealed that activation of the Cpx response has a protective role (Mahoney & Silhavy, 2013).

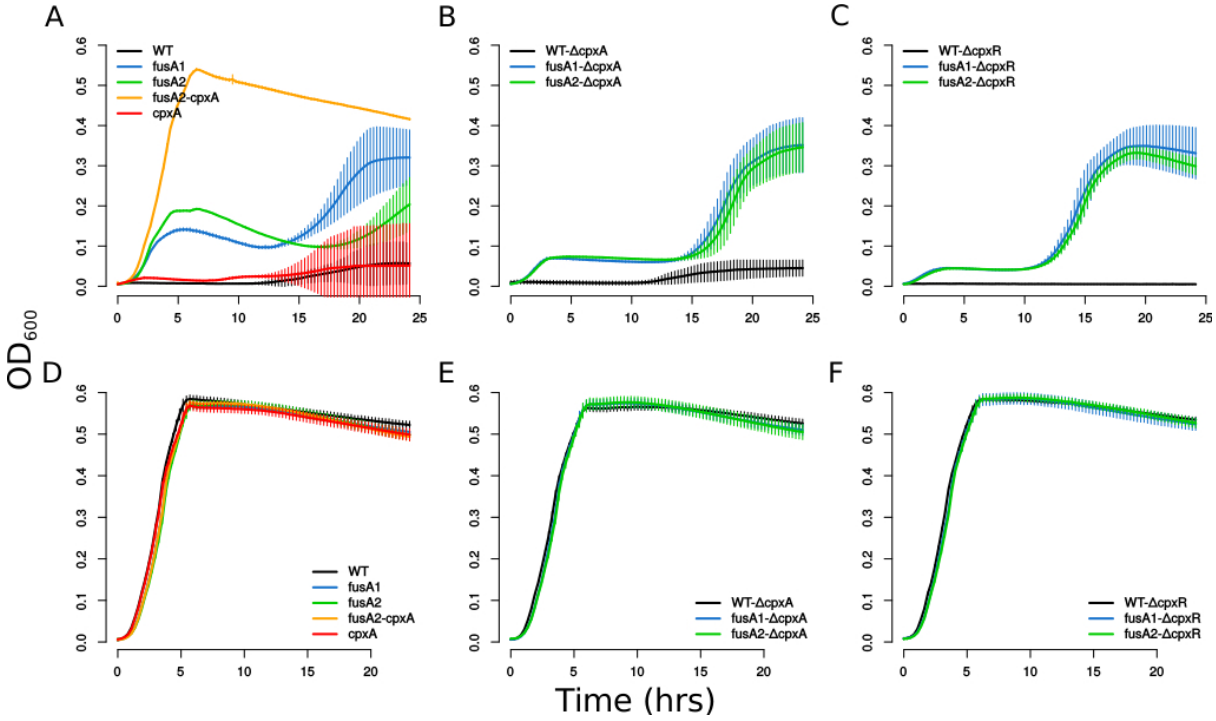

Figure 2: ***Knocking out cpxA/R in the fusA mutants reduces their growth in kanamycin.*** *These are growth experiments. The labels for the x and y axis are common. For brevity, wildtype is denoted by WT, the FusA^{P610T} mutant by fusA1, the FusA^{A608E} mutant by fusA2 the FusA^{A608E}-CpxA^{F218Y} mutant by fusA2-cpxA and the CpxA^{F218Y} mutant by cpxA. Knockouts of cpxA/R are referred to as ΔcpxA/R. Plotted are the means from eight replicates with error-bars representing standard deviation. (A-C) Growth curves in 8-kan. (D-F) Growth curves in 0-kan. FusA$^{P610T/A608E}$-ΔcpxA/R strains do not grow as well as the FusA$^{P610T/A608E}$ or FusA^{A608E}-CpxA^{F218Y} strains in kanamycin. In the 8-kan growth curves the huge error bars in some of the strains are produced when a few replicates start growing, possibly due to acquisition of some resistance conferring mutation, and thus this error cannot be eliminated.*

CpxA has both kinase and phosphatase activities (Raivio & Silhavy, 1997). In the absence of the phosphatase activity of CpxA, CpxR can get phosphorylated by heterologous kinases, resulting in a constitutively activated Cpx response (Raivio & Silhavy, 1997). Thus, knocking out CpxA can result in the activation of the Cpx response and provide resistance (Mahoney & Silhavy, 2013). The Cpx response can also be hyper-activated by point mutations in the periplasmic sensory domain and the second transmembrane helix of CpxA (Raivio & Silhavy, 1997). Mutations in the region next to the predicted autophosphorylation site of CpxA can result in constitutive activation of this sensor kinase (Raivio & Silhavy, 1997). Such hyperactivating mutations protect cells from death in the presence of aminoglycosides (Mahoney & Silhavy, 2013).

To understand the effect of the point mutation in *cpxA* on the activity of the Cpx response, we decided to delete either *cpxA* or *cpxR* in the EF-G mutants to see whether this increased or decreased their growth in kanamycin. Using phage transduction we transferred deletions of either *cpxA* or *cpxR* into FusA^{P610T} and FusA^{A608E} and also to the wildtype as a control. We tested the growth of these strains in the presence and absence of kanamycin. Deletion of either *cpxA* or *cpxR* in the EF-G mutants (FusA^{A608E}-Δ*cpxA*/*R*) resulted in a decrease in growth in kanamycin, while there was no discernible effect of the deletions on the wildtype (Fig. 2A-C). Thus, eliminating the activity of the Cpx system in the EF-G mutants resulted in

a decrease in the ability to grow in kanamycin. This suggests that an intact Cpx response is essential for the resistance of these mutants.

We saw that the FusA^{A608E}-Δ*cpxA*/*R* mutants showed a spurt in growth at a certain point in batch culture, whence these mutants grew better than their EF-G single mutant counterparts (Fig. 2B and C). This was consistent across the different transductants tested (Fig. S7 and S8). However, even after this growth spurt, their saturation optical density never reached that of the FusA^{A608E}-CpxA^{F218Y} double mutant obtained from the evolution experiment (Compare Fig. 2B and C with 2A).

Control growth experiments in the absence of kanamycin told us that the decreased growth of the FusA^{A608E}-Δ*cpxA*/*R* strains seen in kanamycin was not the result of any generic growth defect conferred by the deletions themselves (Fig. 2D-F). Thus, it is reasonable to conclude that the Cpx system is active, and perhaps hyperactive, in the double mutant, and that its activity is linked to resistance. It is notable that knocking out either *cpxA* or *cpxR* had the same effect on growth in kanamycin and that this differs from previously published results where knocking out only *cpxA* and not *cpxR* resulted in increased resistance (Mahoney & Silhavy, 2013). Perhaps in our strain or under our working conditions CpxR may not be getting activated by heterologous kinases.

CpxR has fifty eight targets in RegulonDB (Gama-Castro et al., 2016). However only a handful of these genes are among the differentially regulated genes in the FusA^{A608E}-CpxA^{F218Y} and CpxA^{F218Y} mutants in relation to the wildtype (18 in the CpxA^{F218Y} mutant and 10 in the FusA^{A608E}-CpxA^{F218Y} mutant), as measured by RNA-seq experiments of these mutants in the absence of kanamycin. There are nearly equal numbers of positive and negative targets of CpxR among the up and down-regulated genes. Thus, the status of the Cpx response is not clarified by a bird's eye view of the transcriptome of these mutants. However, *cpxA* and *cpxP* are up-regulated in both the FusA^{A608E}-CpxA^{F218Y} and CpxA^{F218Y} mutants; and *cpxR* is up-regulated in the CpxA^{F218Y} mutant. Among the three, *cpxP* seems to be particularly up-regulated with $\log_2$ fold changes of ~3 in the CpxA^{F218Y} mutant and ~2 in the FusA^{A608E}-CpxA^{F218Y} mutant. On the other hand, the $\log_2$ fold changes of the *cpxA* and *cpxR* genes are between 0.5 and 1. All three genes are positive targets of CpxR. However, CpxP is a periplasmic protein and a negative regulator of the Cpx response (Raivio, Popkin & Silhavy, 1999; Raivio et al., 2000; Fleischer et al., 2007). The higher up-regulation of *cpxP* points to an active Cpx system, and might keep a full blown Cpx response in check. It is possible that in the presence of kanamycin these mutants may be better capable of mounting a protective Cpx response, due to the *degP* mediated degradation of *cpxP* in the presence of misfolded proteins (Isaac et al., 2005).

Further evolution of the FusA^{P610T} mutant in kanamycin reveals *cpxA* as the primary locus targeted for a further increase in resistance.

In our previous evolution experiment, while the FusA^{A608E} mutant rapidly accumulated second site mutations in 8-kan, the FusA^{P610T} mutant which had evolved in 4-kan did not accumulate other mutations even after five transfers (Mogre et al., 2014). Thus we decided to

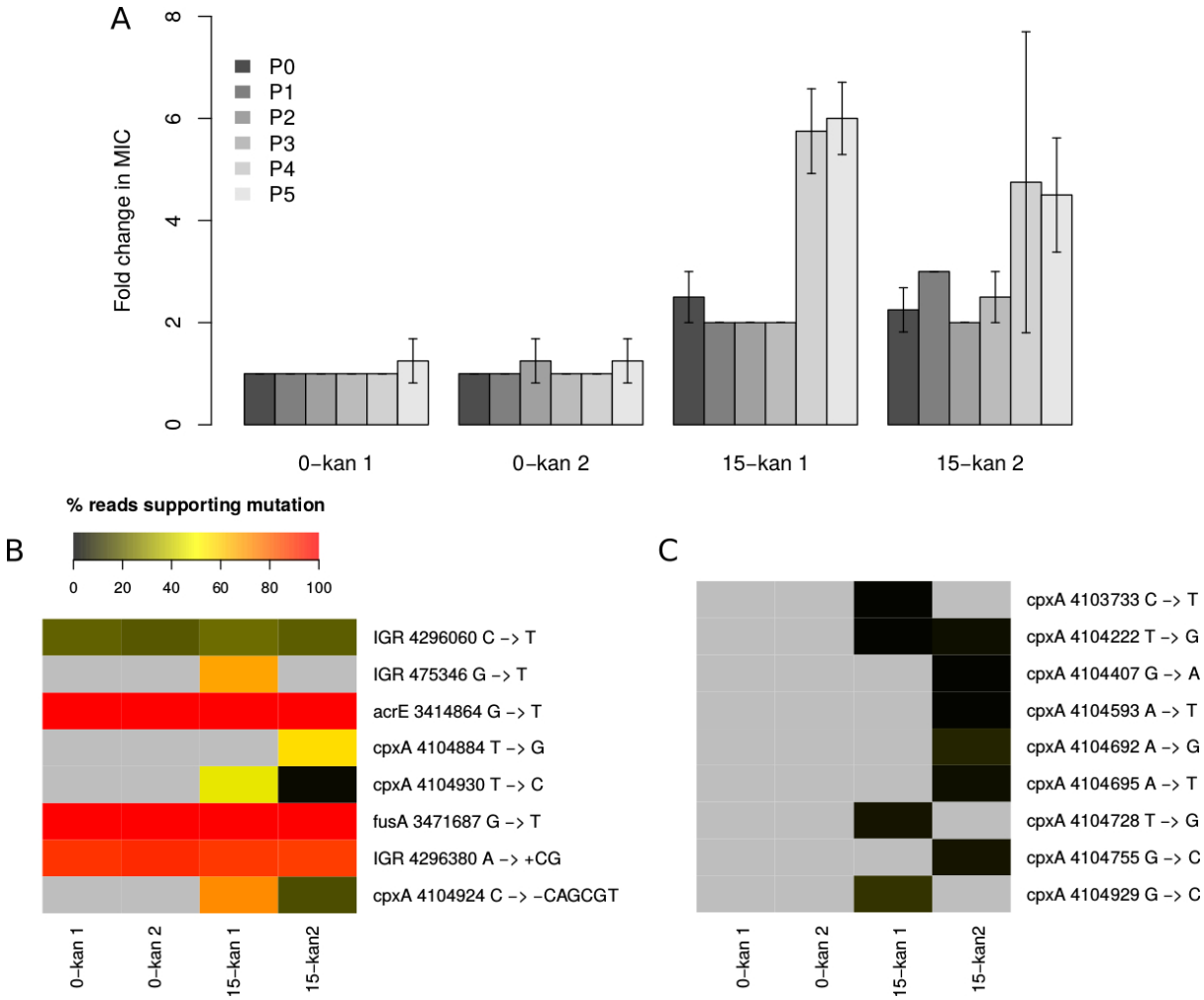

Figure 3: ***Evolution of the FusA^{P610T} mutant in 15-kan yields multiple second site mutations in cpxA.*** *(A) Fold changes in MICs of populations evolved in 15-kan over the MICs of populations evolved in 0-kan. Two replicate populations are shown. MICs of evolving populations at the end of growth (24 hours) after each batch transfer were determined and are represented by P0-P5. The MIC of the 0-kan 1 population at P0 was used to calculate fold changes. MICs of 15-kan populations increased whereas that of the 0-kan populations did not. (B) Heatmaps showing the abundance of variants revealed by sequencing of both control and evolved populations. The colour represents the percentage of reads supporting mutations and is an approximate proxy for the abundance of the mutation. The list of variants was trimmed such that only mutations present in greater than 20% of the reads in at least one sample were retained. Multiple mutations in the gene cpxA are seen in the populations evolved in 15-kan. (C) Heatmaps showing abundance of all low-frequency cpxA variants. The list of variants was trimmed to include only mutations in cpxA. The mutations shown in (B) are not shown here. The colour scale is as shown in (B).*

evolve FusA^{P610T} in a higher concentration of kanamycin (15-kan; 15 µg/ml kanamycin; 25% of the MIC of FusA^{P610T}) to see what second site mutations would accumulate and eventually dominate in the FusA^{P610T} background. The evolution experiment involved serial batch transfers of pure FusA^{P610T} mutant populations in 15-kan every twenty four hours. MICs of all populations were followed at the end of each transfer throughout the experiment.

We observed an initial increase in MIC of around two-fold almost immediately and it notched up further at the end of the fourth transfer to around five to six-fold (Fig. 3A). At the end of the fifth transfer, genomic DNA from both control and evolved populations were

sequenced. We looked at the mutations that were present in at least one sample in greater than 20% frequency (Fig. 3B). In the populations evolved in 15-kan we saw multiple different mutations in *cpxA* present in different frequencies. There were two point mutations and one deletion of 6 nucleotides in *cpxA*. In the unfiltered list of mutations we saw more mutations in *cpxA* that were present at low frequencies only in the populations evolved in kanamycin (Fig. 3C). Thus we see a heterogeneous population with different mutations in *cpxA*. This heterogeneity might be responsible for the large variations in the MIC determinations of these populations (Fig. 3A).

Residue changes in CpxA that confer kanamycin resistance were scattered across the protein and were located in helix-I, periplasmic and cytoplasmic-II domains (Fig. S9). In particular, mutations in helix-I reached high frequencies (>50%) in the FusA^{P610T} populations evolved in 15-kan. The residue T16 in helix-I was particularly targeted with three different mutations, two of which reached high frequencies. Mutations in the periplasmic domain, helix-II and cytoplasmic-II domain are known to result in kanamycin resistance due to hyperactivation of CpxA (Raivio & Silhavy, 1997). However, we did not see any mutations in helix-II.

We noticed that multiple low frequency mutations in the gene *sbmA* had appeared in the populations evolved in kanamycin (Fig. S10). The product of this gene is involved in the transport of peptide antibiotics and its deletion results in increase of resistance to antimicrobial peptides (Laviña, Pugsley & Moreno, 1986; Yorgey et al., 1994; Salomón & Farías, 1995; Saier et al., 2009; Corbalan et al., 2013; Runti et al., 2013; Paulsen et al., 2016).

To summarize, the *cpxA* locus seems to be the primary region targeted for the next significant increase in resistance of the EF-G point mutant.

Disruption of adenylate cyclase catalytic activity gives kanamycin resistance mediated by altered CRP function.

Adenylate cyclase is an enzyme that catalyzes the synthesis of cyclic adenosine monophosphate (cAMP) from ATP. cAMP functions as a second messenger in *E. coli* (Botsford & Harman, 1992; McDonough & Rodriguez, 2012). A well-known mechanism by which cAMP alters gene expression is by binding to and allosterically activating the global transcription regulator cAMP receptor protein (CRP) (Botsford & Harman, 1992; McDonough & Rodriguez, 2012), which has 477 targets in RegulonDB. Girgis et al., subsequent to a transposon mutagenesis screen, demonstrated that deletions of *cyaA* and *crp* increased resistance to aminoglycosides (Girgis, Hottes & Tavazoie, 2009). Furthermore, inactivation of adenylate cyclase was shown to result in activation of the Cpx system (Strozen, Langen & Howard, 2005) which has a known role to play in kanamycin resistance (Mahoney & Silhavy, 2013).

Thus, we wanted to understand the impact of the CyaA^{N600Y} allele, evolved during growth in kanamycin, on the activity of adenylate cyclase. We found that the level of cAMP in both the CyaA^{N600Y} and FusA^{A608E}-CyaA^{N600Y} mutants was lower than that in the wildtype and comparable to that in Δ*cyaA* (Fig. 4). Thus, the CyaA^{N600Y} mutation results in a loss of

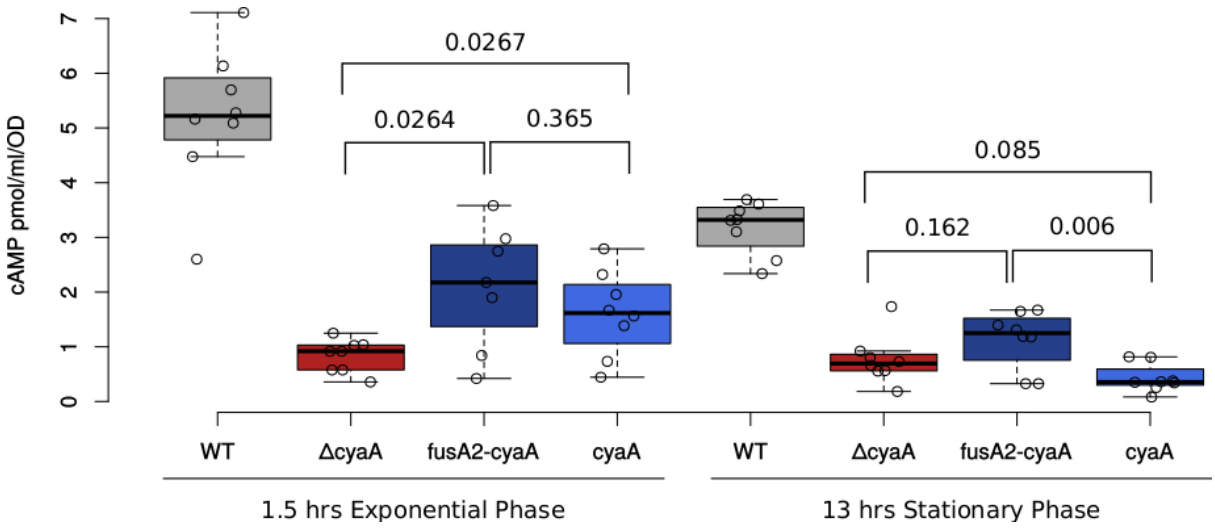

Figure 4: ***cAMP levels in the FusA^{A608E}-CyaA^{N600Y} and CyaA^{N600Y} are lower than that of the wildtype.*** *Boxplots showing the distribution of cAMP estimates. The mutants are referred to by their gene names for brevity. Estimations were done in both the exponential and stationary phase and the results are similar. The difference between the wildtype and the other mutants are significant (P value < 1 x 10^{-2}). P values for other relevant comparisons are mentioned in the plot. The FusA^{A608E}-CyaA^{N600Y} mutant is referred to as fusA2-cyaA and the CyaA^{N600Y} mutant as cyaA.*

catalytic activity. The greater spread in the cAMP levels in the CyaA^{N600Y} and FusA^{A608E}-CyaA^{N600Y} mutants suggests that the mutated adenylate cyclase might have reduced catalytic activity, and not a complete loss of function. This is consistent with the fact that this mutation is present in the regulatory domain of the protein and not the catalytic domain.

As an additional check we transferred the Δ*cyaA* knockout into the FusA$^{P610T/A608E}$ mutants and the wildtype using phage transduction. We were able to see an increase in the stationary phase cell density of the FusA$^{P610T/A608E}$-Δ*cyaA* strains in kanamycin whereas WT-Δ*cyaA* was not affected considerably (Fig. 5A and B).

To understand if this process was mediated by CRP, we also transferred Δ*crp* into the FusA$^{P610T/A608E}$ mutants and the wildtype using phage transduction. These FusA$^{P610T/A608E}$-Δ*crp* strains were also able to grow to a better stationary phase cell density in kanamycin, whereas the WT-Δ*crp* was not (Fig. 5C). Both these observations were consistent across multiple transductants tested (Fig. S11).

Both the Δ*cyaA* and Δ*crp* deletion strains, in the FusA$^{P610T/A608E}$ mutant backgrounds, had a lower growth rate in kanamycin compared to FusA$^{P610T/A608E}$ and FusA^{A608E}-CyaA^{N600Y}. The presence of a similar growth defect in the wildtype strain containing these gene knockouts, during growth in the absence of kanamycin, indicated that the growth defect was specific to the gene knockouts (Fig. 5D-F and S12). The absence of this growth defect in the CyaA^{N600Y} and FusA^{A608E}-CyaA^{N600Y} mutants (Fig. 5D) again suggests that the point mutation in *cyaA* does not result in a complete loss of function in adenylate cyclase. Thus we conclude that the evolved point mutation in *cyaA* results in kanamycin resistance via an altered adenylate

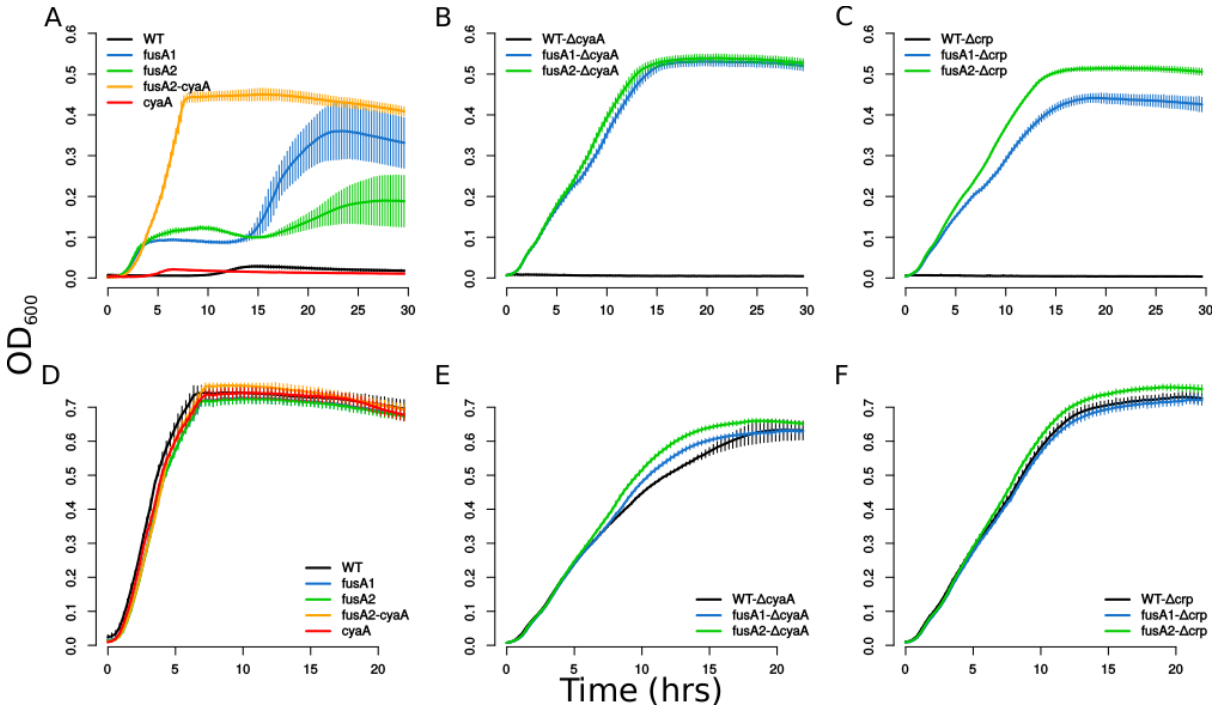

Figure 5: ***Knocking out cyaA / crp in the fusA mutants increases their growth in kanamycin.*** *These are growth experiments. The labels for the x and y axis are common. For brevity, wildtype is denoted by WT, the FusA^{P610T} mutant by fusA1, the FusA^{A608E} mutant by fusA2 the FusA^{A608E}-CyaA^{N600Y} mutant by fusA2-cyaA and the CyaA^{N600Y} mutant by cyaA. Knockouts of cyaA / crp are referred to as* Δcya*A*/ Δcrp. *Plotted are the means from eight replicates with error-bars representing standard deviation. (A-C) Growth curves in 8-kan. (D-F) Growth curves in 0-kan. FusA$^{P610T/A608E}$-Δ*cyaA*/Δ*crp strains have better growth in kanamycin than the FusA$^{P610T/A608E}$ strains. In the 8-kan growth curves the huge error bars in some of the strains are produced when a few replicates start growing, possibly due to acquisition of some resistance conferring mutation, and thus this error cannot be eliminated.*

cyclase and subsequently altered CRP function. This mutation has the added benefit of not conferring the growth defect associated with the knockouts of either of these genes.

We next compared the transcriptomes of the CyaA^{N600Y} mutant with the transcriptomes of the Δ*cyaA* and Δ*crp* strains. Surprisingly, fold changes of genes in CyaA^{N600Y}, in comparison to the wildtype, negatively correlated with those in the Δ*crp* and Δ*cyaA* strains (Fig. 6A and B). This correlation was low but significant. This is consistent with the results of our comparison with the list of CRP targets available in the RegulonDB database. As expected, genes that are activated by cAMP-CRP are down-regulated in the Δ*cyaA* and Δ*crp* strains (Fig. 6C). However such genes are mostly up-regulated in the CyaA^{N600Y} mutant (Fig. 6C). Thus, though the list of differentially expressed genes overlaps with the list of CRP targets, the nature of differential expression is opposite to that expected. This stands for the FusA^{A608E}-CyaA^{N600Y} mutant as well (Fig. S13).

Thus although the levels of cAMP are low in the CyaA^{N600Y} mutant (Fig. 4), their transcriptomes are opposite to that of Δ*cyaA* / Δ*crp* (Fig. 6). This is contradictory to expectation, more so since since the FusA$^{P610T/A608E}$-Δ*cyaA* / Δ*crp* strains grow better in kanamycin than the FusA$^{P610T/A608E}$ mutants. It is possible that this phenotypic similarity of the FusA$^{P610T/A608E}$-Δ*cyaA* / Δ*crp* strains to the FusA^{P610T}-CyaA^{N600Y} mutant is coincidental and

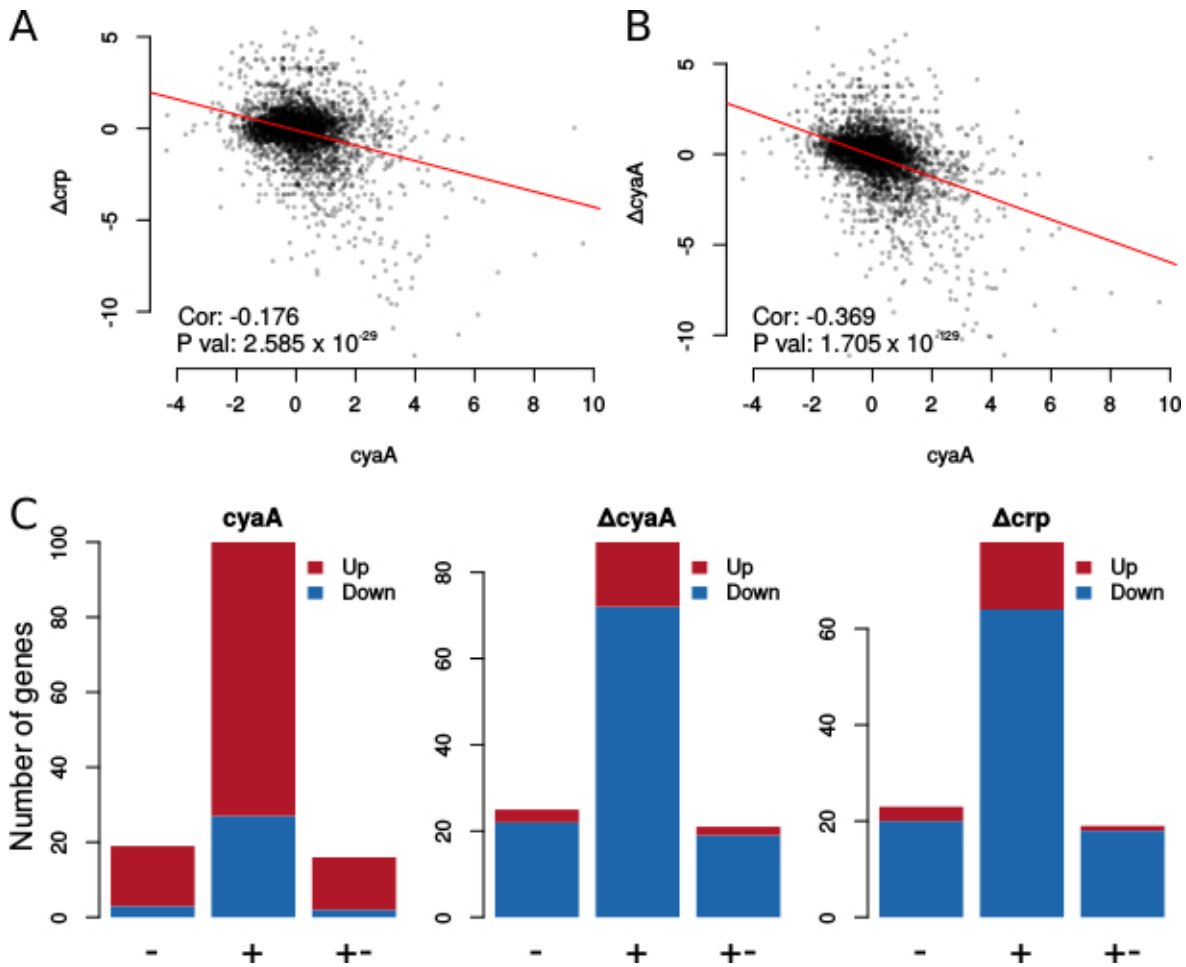

Figure 6: ***The transcriptome of the CyaA^{N600Y} mutant is opposite to that of the Δcrp / ΔcyaA strains.*** *(A-B) Scatter plots comparing Log$_2$ fold-changes of genes in the CyaA^{N600Y} mutant with those in the Δcrp (A) / ΔcyaA (B) knockout strains. The mutant is referred to by its gene name for brevity. Fold changes in the Δcrp / ΔcyaA strains were calculated as for the other mutants. The time-points for cell harvesting for RNA extraction of the ΔcyaA / Δcrp strains were also similar. Fold changes of genes in the CyaA^{N600Y} mutant correlates negatively with fold changes of genes in ΔcyaA / Δcrp strains. The strength of the Spearman correlation coefficient is low but significant as can be seen from the P values; both are mentioned in the plot. (C) This opposite behaviour of the CyaA^{N600Y} mutant is also clear from the number of targets of CRP present in the up and down-regulated genes. The numbers of positive (+), negative (-) and dual targets (+-) of CRP present among the up (red) and down-regulated (blue) genes are shown in the stacked barplots. The strain is mentioned over each barplot. Many positively regulated targets of CRP are down-regulated among the ΔcyaA / Δcrp strains, as can be expected from the absence of the activator (cAMP-CRP) of these genes. However, the opposite is seen in the CyaA^{N600Y} mutant, where many positively regulated targets of CRP are up-regulated. Similar results are seen with the FusA^{A608E}-CyaA^{N600Y} mutant and are shown in Fig. S13.*

that the full knockout and the point mutant confer resistance through distinct means. This might however explain why we do not see the growth defect associated with Δ*cyaA* / Δ*crp* in the CyaA^{N600Y} mutant.

This unexpected behaviour of the CyaA^{N600Y} mutation could stem from the fact that the CyaA^{N600Y} mutation is a point mutation and not a knockout. As a result, the adenylate cyclase protein would still be produced, and this could have alternative functions. There could also

be feedback involved: although not called up-regulated, the fold changes of both *cyaA* and *crp* are higher by around 2-fold in the CyaA^{N600Y} and FusA^{A608E}-CyaA^{N600Y} mutants (Fig. S14). In line with this, the promoter activities of these two genes were also higher in the CyaA^{N600Y} mutant (Fig. S14A and B), as revealed by promoter-GFP fusions. Thus, further work is required to understand the function of CyaA^{N600Y}.

Transcriptome of the FusA^{A608E}-TopA^{S180L} mutant shows evidence for supercoiling mediated transcriptional changes.

The bacterial chromosome is a highly condensed and supercoiled DNA molecule (Woldringh, 2002; Thanbichler, Wang & Shapiro, 2005; Thanbichler & Shapiro, 2006; Toro & Shapiro, 2010). The extent of supercoiling can influence gene expression (Travers & Muskhelishvili, 2005), and is known to be affected by various environmental factors (Rui & Tse-Dinh, 2003) such as osmotic stress (McClellan et al., 1990; Cheung et al., 2003), starvation (Balke & Gralla, 1987), temperature (McClellan et al., 1990) and oxygen tension (Hsieh, Burger & Drlica, 1991). Global supercoiling of the chromosome is maintained by a balance between the activities of enzymes called topoisomerases. DNA gyrase (Topoisomerase II, encoded by the genes *gyrA* and *gyrB*) catalyzes an increase in negative superhelicity. Topoisomerases I (*topA*), III (*topB*) and IV (*parC* and *parE*) relax negative supercoils (Travers & Muskhelishvili, 2005; Gubaev & Klostermeier, 2014). Topoisomerase IV can also relax positive supercoils, which is its preferred substrate (Crisona et al., 2000) and is involved in decatenation and unknotting of DNA (López et al., 2012). The decatenation activity is triggered by an increase in negative supercoiling (Zechiedrich, Khodursky & Cozzarelli, 1997). The levels of these enzymes in the cell are maintained by a homeostatic feedback from the supercoiled state of the chromosome (Menzel & Gellert, 1987; Tse-Dinh & Beran, 1988; Pruss & Drlica, 1989; Snoep et al., 2002).

Antibiotics, for example novobiocin and norfloxacin, that block the activities of supercoiling genes have been used to study the resulting effects on gene expression (Peter et al., 2004). Subunits of DNA gyrase and Topoisomerase IV are homologous (Kato et al., 1990) and perhaps as a result antibiotics that target one also end up targeting the other (Bellon et al., 2004). There are however preferences: novobiocin's primary target is DNA gyrase and its secondary target is Topoisomerase IV (Hardy & Cozzarelli, 2003; Bellon et al., 2004), whereas, norfloxacin primarily inhibits the activity of Topoisomerase IV and as a secondary target, the activity of DNA gyrase (Fournier et al., 2000). Thus, inhibition by novobiocin should result in decreased negative supercoiling in the cell, as a consequence of loss of DNA gyrase function (Peter et al., 2004). Inhibition by norfloxacin would result in an increase in positive supercoils as a consequence of the inhibition of Topoisomerase IV, the antibiotic's primary target (Peter et al., 2004). Norfloxacin treatment will also result in decreased negative supercoils as a consequence of the inhibition of its secondary target, DNA gyrase (Peter et al., 2004).

One of the second site mutations in the FusA^{A608E} mutant lies in Topoisomerase I (TopA^{S180L}). Thus we were interested in understanding the effect of the point mutation on the activity of Topoisomerase I. For this reason we analysed the transcriptome of the FusA^{A608E}-TopA^{S180L}

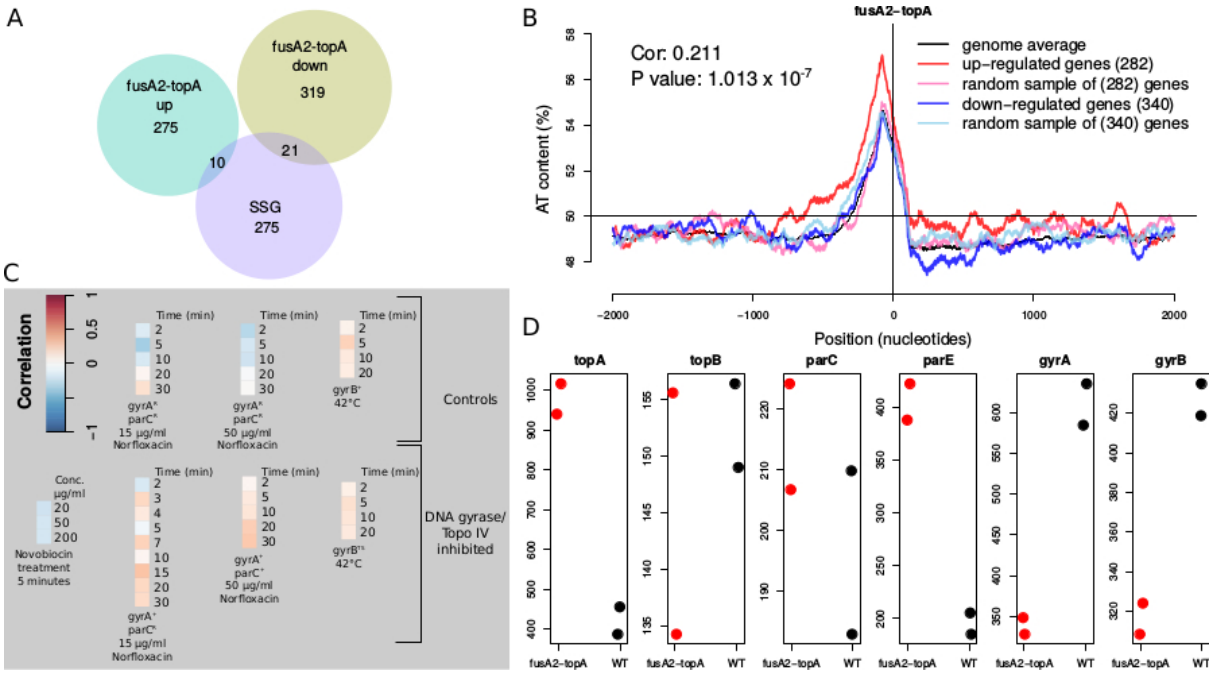

Figure 7: ***Evidence for supercoiling changes in the FusA^{A608E}-TopA^{S180L} mutant.*** *(A) Venn diagram showing overlaps between up / down-regulated genes in the FusA^{A608E}-TopA^{S180L} mutant (fusA2-topA) with the list of supercoiling sensitive genes given by Peter et al. (Peter et al., 2004). Overlaps are small and not significant. (B) Up-regulated genes in the FusA^{A608E}-TopA^{S180L} mutant are AT rich. The mean AT contents of up / down-regulated genes are shown. AT contents were calculated using a 100 basepair moving window, moving by a basepair, +/- 2kb the start site of the gene. The mean AT contents of all genes in the genome are plotted in black. Mean AT contents of up-regulated genes are plotted in red, whereas mean AT contents of down-regulated genes are plotted in blue. Mean AT contents of a random sample of genes equal to the number of up / down-regulated genes in that sample are plotted in a lighter shade of the respective colour. The Spearman correlation coefficient of differentially expressed gene AT contents with fold changes of these genes, and the corresponding P value for the correlation are mentioned in the plot. The AT contents of up-regulated genes is higher than the genomic average in this mutant. (C) Correlations of fold changes of genes in the FusA^{A608E}-TopA^{S180L} with microarray derived gene-expression ratios obtained by inhibiting DNA gyrase function (Peter et al., 2004). Antibiotics that target DNA gyrase, as well as temperature sensitive mutants were used to achieve DNA gyrase inhibition and hence chromosomal relaxation. The two antibiotics used were Norfloxacin and Novobiocin. When used on the wildtype strain, these antibiotics result in DNA gyrase (gyrA and gyrB) / Topoisomerase IV (parC and parE) inhibition. Resistant strains serve as controls. Strains resistant to Novobiocin have not been used. Two different concentrations of Norfloxacin were used and they provide similar results. Wildtype genes are indicated by + and resistant strains with the R superscript. Inhibition of the temperature sensitive DNA gyrase was obtained at 42 °C. Wildtype DNA gyrase serves as the control. The temperature sensitive gene is represented with a TS superscript. Strength of correlation is indicated by colour and is shown in the key. (D) RPKM values of supercoiling genes are changed in the FusA^{A608E}-TopA^{S180L} mutant. Gene names are mentioned over each plot. The mutant is referred to by gene names for brevity and wildtype with the FRT site introduced near fusA as WT. Since two replicates were sequenced there are only two points for comparison.*

mutant for similarities with supercoiling related effects. From our analysis, we suggest that the mutation results in a functionally reduced Topoisomerase I.

Peter et al. used supercoiling gene targeting antibiotics and temperature sensitive DNA gyrase mutants to change the supercoiling of the *E. coli* chromosome, and profile the

resulting changes in the transcriptome using microarrays (Peter et al., 2004). Their data consists of gene expression ratios obtained from microarrays, loaded with RNA from cells at multiple timepoints after treatment / temperature shift, with RNA from cells before treatment / temperature shift serving as a reference. By analysing all their datasets together, they constructed a list of supercoiling-sensitive genes. We see little overlap with these genes (Fig. 7A). They also show that relaxation induced genes are AT-rich. Although we see that up-regulated genes in the FusA^{A608E}-TopA^{S180L} mutant are AT-rich (Fig. 7B, compare with other mutants in Fig. S15), these do not overlap with the list of relaxation-induced genes identified by Peter and colleagues (Peter et al., 2004).

Next we looked at correlations of fold changes of genes in the FusA^{A608E}-TopA^{S180L} mutant with the gene expression ratios across each condition in the Peter et al. dataset. We found that the FusA^{A608E}-TopA^{S180L} mutant negatively correlates with novobiocin treatment (Fig. 7C). Negative correlation with novobiocin treatment suggests that there is increased negative supercoiling in the cell, since novobiocin inhibits DNA gyrase. This view is supported by the expression levels of the topoisomerases themselves (Fig. 7D). As expected from negative feedback in the presence of high negative supercoiling, the levels of *gyrA* and *gyrB* (DNA gyrase) are low and that of *topA* (Topoisomerase I) is high (Fig. 7D).

Inhibition of TopA results in hyper-negative supercoiling (Stupina & Wang, 2005). Thus these lines of evidence suggest that the mutation in *topA* reduces its activity and results in increased negative supercoiling in the cell due to intact DNA gyrase function. The FusA^{A608E}-TopA^{S180L} mutant shows a slight growth defect at a lower temperature (Fig. S16), which is in line with the known cold sensitivity of the *topA* deletion strain (Stupina & Wang, 2005). We do not not know the extent to which its activity is compromised due to the mutation. The loss in activity could also result in increased R-loop formation in the mutant since Topoisomerase I resolves R-loops (Massé & Drolet, 1999; Usongo et al., 2008). Increased translation may help reduce R-loops (Massé & Drolet, 1999; Broccoli et al., 2004; Gowrishankar & Harinarayanan, 2004; Gowrishankar, Leela & Anupama, 2013). This might even potentially explain the possible genetic interaction between *fusA* and *topA*. Increased dosage of genes encoding Topoisomerase IV (*parC* and *parE*) have been shown to relieve growth defects caused by inactivation of *topA* (Kato et al., 1990). We also see an increased expression of *parC* and *parE* in the FusA^{A608E}-TopA^{S180L} mutant (Fig. 7D).

The FusA^{A608E}-TopA^{S180L} mutant, somewhat contradictorily, positively correlates with norfloxacin treatment (Fig. 7C). This is more difficult to interpret in the light of the effects of norfloxacin on Topoisomerase IV as well. Since Topoisomerase IV relaxes positive supercoils, it is possible that there is increased positive supercoiling as well in the mutant, thus resulting in positive correlation with norfloxacin treatment. This will indicate variation in the effect of the mutant on local superhelicity along the chromosome. This interpretation is complicated by the fact that the positive correlation persists even in norfloxacin-treated cells carrying a Topoisomerase IV variant that is resistant to the antibiotic (Fig. 7C); as well by our understanding that TopA is unable to relax positively supercoilied templates. The FusA^{A608E}-TopA^{S180L} mutant also positively correlated with both their wildtype gyrase and a

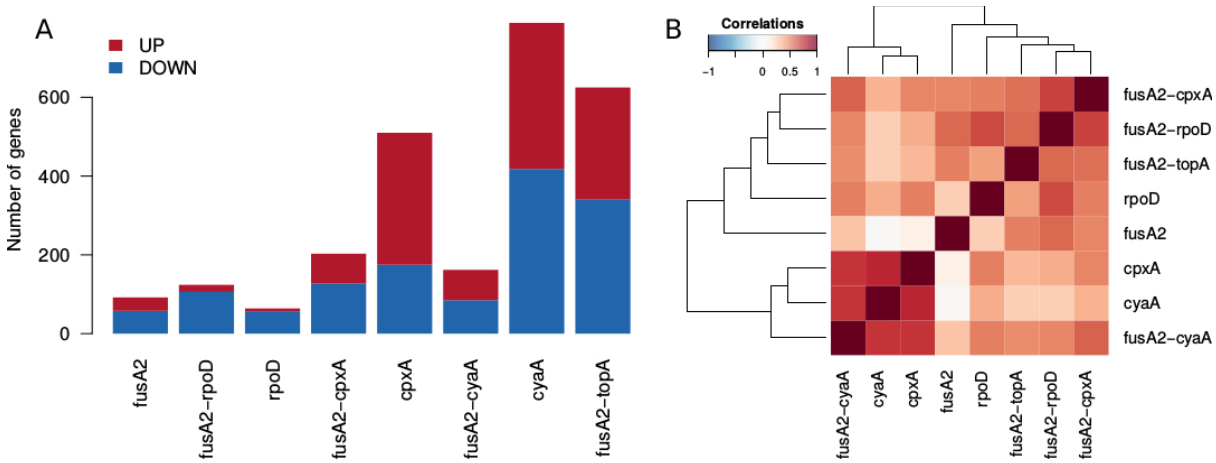

Figure 8: ***Summary of differentially expressed genes across mutants.*** *(A) Numbers of up and down-regulated genes in the mutants. Mutants are referred to by their gene names for brevity. (B) Heatmap showing the matrix of Spearman correlations among mutants. Fold changes of all genes were used to derive these correlations.*

temperature sensitive gyrase grown at 42°C and thus it is difficult to draw conclusions from these comparisons (Fig. 7C).

There is low correlation between the novobiocin and norfloxacin treatments within the Peter et al. dataset, indicating that their effects can be rather different from each other (Fig. S17). Thus, the fact that the FusA^{A608E}-TopA^{S180L} mutant shows weak, yet opposing correlations between the two comparisons is not necessarily an internally inconsistent observation. In the Peter et al. dataset, *E. coli* with Topoisomerase IV that is sensitive to norfloxacin transcriptionally responds in a manner similar to one with a variant that is resistant to the antibiotic (Fig. S17). This complicates our understanding of the role of Topoisomerase IV activity in gene expression.

To our knowledge, we are the first to explore the link between chromosomal supercoiling and aminoglycoside resistance. There is some evidence for a change in supercoiling in the FusA^{A608E}-TopA^{S180L} mutant. The evidence is conflicting especially in the case of correlations of the mutant with norfloxacin and novobiocin treatments. Since we do not have a TopA^{S180L} single mutant we don't understand the effects of the FusA^{A608E} mutation on the TopA^{S180L} mutation. Further experiments will help work out the biochemical activity of the TopA^{S180L} mutant, its genetic interaction with FusA^{A608E}, and the mechanism of resistance of this mutant.

Similarities among mutants

The number of differentially expressed genes varied substantially among the mutants (Fig. 8A). The CpxA^{F218Y}, CyaA^{N600Y} and FusA^{A608E}-TopA^{S180L} mutants had the most number of differentially expressed genes. The FusA^{A608E}, RpoD^{L261Q} and FusA^{A608E}-RpoD^{L261Q} mutants had the least number of differentially expressed genes.

We were surprised that the *rpoD* mutants had the least number of differentially expressed genes considering the role of this gene as a transcription initiation factor for around 50% of

the genes in *E. coli*, particularly those expressed in exponentially growing cells. How this mutation results in resistance remains elusive. Nonetheless, the location of the mutation is interesting. The mutation resides in a highly conserved residue in the large non-conserved domain of this protein (Fig. S18). While no clear function is ascribed to this domain, certain residues in this domain have been shown to be involved in promoter escape (Leibman & Hochschild, 2007), and one of these residues lies very close to the mutated residue mentioned in our study. It is difficult to hypothesise how a residue involved in allowing the escape of the RNA polymerase from the housekeeping sigma factor to facilitate transcription initiation, must be involved in aminoglycoside resistance, but in the absence of other information remains a valuable lead.

Clustering based on correlation between fold changes of all genes relative to the wildtype across mutants tends to cluster the dataset according to the mutants, but not always so (Fig. 8B). Notably, fold changes of differentially expressed genes in the CyaA^{N600Y} mutant are well correlated with that in the CpxA^{F218Y} mutant. Thus, as an outcome of the evolution experiment, we see two different mutations resulting in a similar transcriptome, i.e., two different ways of achieving the same net effect. Correlations of fold changes of genes in the FusA^{A608E}-CyaA^{N600Y} mutant with CyaA^{N600Y} and CpxA^{F218Y} mutants were high, however, those between the FusA^{A608E}-CpxA^{F218Y} mutant and either CyaA^{N600Y} or CpxA^{F218Y} mutants were lower. The correlation between the FusA^{A608E}-CpxA^{F218Y}, FusA^{A608E}-RpoD^{L261Q} and FusA^{A608E}-TopA^{S180L} mutants were high, offering another example of converging effects of different mutations.

Effect of second site mutants on gene expression and dependence on EF-G

We evaluated the impact of the FusA^{A608E} mutation on the transcriptomes of the double mutants in detail. The FusA^{A608E} single mutant had roughly thirty genes up and fifty genes down-regulated (Fig. 8A). Sequencing of the transcriptomes of single and double mutants enabled us to look at interactions of the FusA^{A608E} mutant with the second site mutations in terms of fold changes of differentially expressed genes. From the transcriptomes of exponentially growing cells, we saw clear interactions of the primary kanamycin resistance conferring mutation in *fusA* with the second site mutations in *cyaA*, *cpxA* and *rpoD*.

To assess the extent to which the transcriptomes of the FusA^{A608E} single mutant and CyaA^{N600Y} / CpxA^{F218Y} / RpoD^{L261Q} single mutants explain the gene expression state of the FusA^{A608E}-CyaA^{N600Y} / CpxA^{F218Y} / RpoD^{L261Q} double mutants, we plotted the $\log_2$ fold change in the double mutant against the sum of the $\log_2$ fold changes in the FusA^{A608E} single mutant and the second site single mutants (Fig. S19D, H and L). In the absence of a genetic interaction between the two single mutants, we would expect the scatter plot to lie along the 45° line. We find that this is not the case in each of the three double mutants we evaluated. In other words, the absolute difference in $\log_2$ fold change in expression between the double mutant and the sum of the two corresponding single mutants is significantly different from zero (Wilcoxon signed rank test P value < 2.2×10^{-16}, Fig. S19). These indicate that the FusA^{A608E} background affects the transcriptional state of the CyaA^{N600Y} / CpxA^{F218Y} / RpoD^{L261Q} single mutants in a non-additive manner.

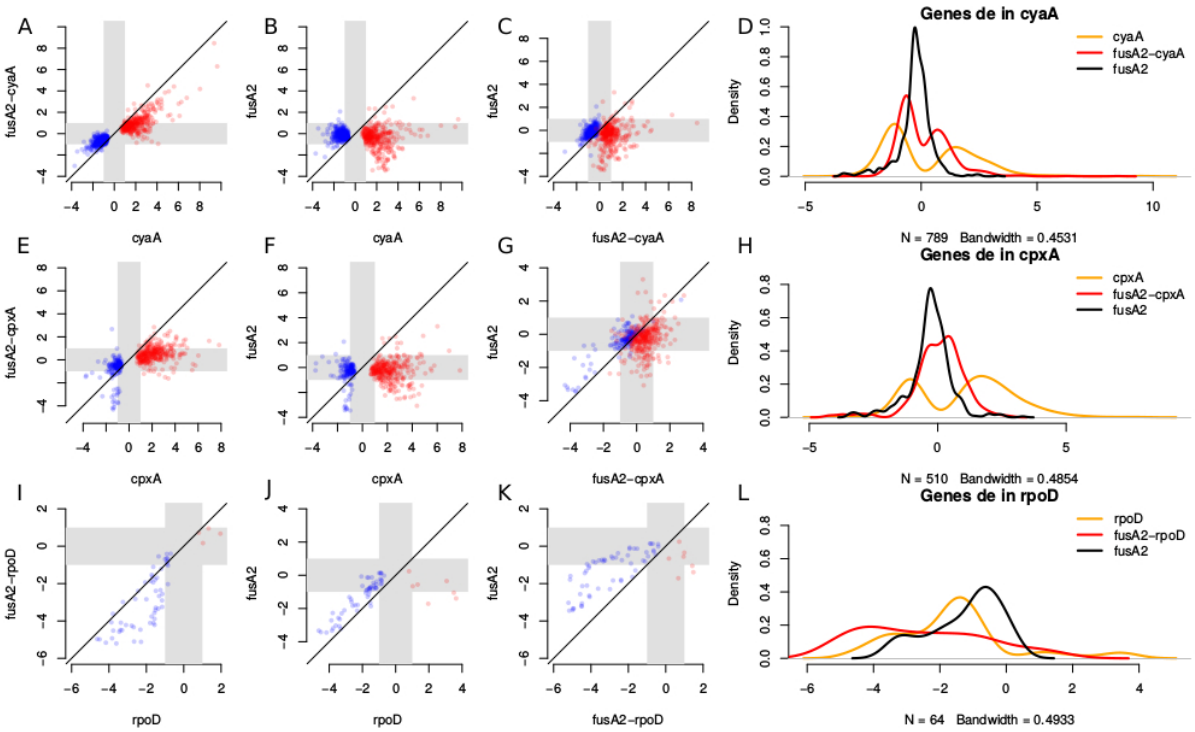

Figure 9: ***Effect of second site mutations on gene expression and dependence on EF-G.*** *(A-C, E-G, I-K) Scatter plots comparing log_2 fold changes of differentially expressed genes among mutants. Mutants are referred to by their gene names for brevity. Grey zones indicate the region between the log_2 fold changes of +1 and -1 (corresponding to fold changes of 2 and 0.5), and thus highlights the region of low / no fold change. (D, H and L) are kernel density plots (smoothed histograms) that show distributions of log_2 fold changes of differentially expressed genes in mutants. (A-D) Fold changes of genes differentially expressed in the CyaA^{N600Y} mutant were compared in the FusA^{A608E}-CyaA^{N600Y} and FusA^{A608E} mutants. Red points show genes up-regulated genes and blue points show genes down-regulated in the CyaA^{N600Y} single mutant. (A) Many genes above the log_2 fold change threshold of +/- 1 in the CyaA^{N600Y} mutant are below that threshold in the FusA^{A608E}-CyaA^{N600Y} mutant. (B and C) Most of these genes are not differentially expressed in the FusA^{A608E} mutant. (D) The density plot summarises these results to show that genes differentially expressed in the CyaA^{N600Y} mutant are not differentially expressed in the FusA^{A608E} mutant, and have intermediate fold changes in the FusA^{A608E}-CyaA^{N600Y} mutant. (E-H) Fold changes of genes differentially expressed in the CpxA^{F218Y} mutant were compared in the FusA^{A608E}-CpxA^{F218Y} and FusA^{A608E} mutants. Red points show genes up-regulated genes and blue points show genes down-regulated in the CpxA^{F218Y} single mutant. (E) Many genes above the log_2 fold change threshold of +/- 1 in the CpxA^{F218Y} mutant are below that threshold in the FusA^{A608E}-CpxA^{F218Y} mutant. (F and G) Most of these genes are not differentially expressed in the FusA^{A608E} mutant. (H) The density plot summarises these results to show that genes differentially expressed in the CpxA^{F218Y} mutant are not differentially expressed in the FusA^{A608E} mutant, and have intermediate fold changes in the FusA^{A608E}-CpxA^{F218Y} mutant. Although from the density plots it seems like these gene are not differentially expressed in the FusA^{A608E}-CpxA^{F218Y} mutant, from the separation between the up and down-regulated genes seen in (G), it is clear that fold changes are intermediate. (I-L) Fold changes of genes differentially expressed in the RpoD^{L261Q} mutant were compared in the FusA^{A608E}-RpoD^{L261Q} and FusA^{A608E} mutants. Red points show genes up-regulated genes and blue points show genes down-regulated in the RpoD^{L261Q} single mutant. (I) Many down-regulated genes in the RpoD^{L261Q} mutant are further down-regulated in the FusA^{A608E}-RpoD^{L261Q} mutant. The up-regulated genes in the RpoD^{L261Q} mutant are less up-regulated in the FusA^{A608E}-RpoD^{L261Q} mutant (J and K) Many of the down-regulated genes in the RpoD^{L261Q} mutant are also down-regulated in the FusA^{A608E} mutant whereas the up-regulated genes in the RpoD^{L261Q} mutant are not up-regulated in the FusA^{A608E} mutant (D) The density plot summarises these results to show that genes down-regulated in the RpoD^{L261Q} mutant are further down-regulated in the FusA^{A608E}-RpoD^{L261Q} mutant. Many of these genes are also down-regulated in the FusA^{A608E} mutant.*

More specifically, we saw that the fold changes of genes differentially expressed in the CyaA^{N600Y} mutant were reduced in the FusA^{A608E}-CyaA^{N600Y} mutant (Fig. 9A). Most of these genes were not differentially expressed in the FusA^{A608E} mutant (Fig. 9B and C). This result is summarized in the kernel density plot (Fig. 9D) which shows that these genes have extreme fold changes in the CyaA^{N600Y} mutant, low or no fold change in the FusA^{A608E} mutant and intermediate fold changes in the FusA^{A608E}-CyaA^{N600Y} mutant.

We saw that this was the case with the CpxA^{F218Y} and FusA^{A608E}-CpxA^{F218Y} mutants as well (Fig. 9E-H). As a result of this, the number of differentially expressed genes in the FusA^{A608E}-CyaA^{N600Y} or FusA^{A608E}-CpxA^{F218Y} mutants is lesser than that in the CyaA^{N600Y} or CpxA^{F218Y} mutants (Fig. 8A). The effect of the mutation in *fusA* on the fold changes of genes seems to be more extreme in the case of the mutation in *cpxA* than *cyaA*, since FusA^{A608E}-CpxA^{F218Y} does not correlate as well with CpxA^{F218Y} as does FusA^{A608E}-CyaA^{N600Y} with CyaA^{N600Y} (Fig. 8B).

These observations bear in part from the fact that the fold changes of genes differentially expressed in the CyaA^{N600Y} and CpxA^{F218Y} mutants are opposite to the fold changes of these genes in the FusA^{A608E} mutant (Fig. S20A and B), even though they were not classified as differentially expressed in FusA^{A608E}. In other words, a gene that is up-regulated in CyaA^{N600Y} / CpxA^{F218Y} displays a mild negative fold change in FusA^{A608E}; whereas one that is down-regulated in the former shows a slight positive fold change in the latter (Fig. S20A and B).

We notice that the effect of FusA^{A608E} on RpoD^{L261Q} is opposite to that on CyaA^{N600Y} / CpxA^{F218Y}. Genes down-regulated in the RpoD^{L261Q} mutant were further down-regulated in the FusA^{A608E}-RpoD^{L261Q} mutant (Fig. 9I-L). In this case, many down-regulated genes in RpoD^{L261Q} or FusA^{A608E}-RpoD^{L261Q} were also down-regulated in the FusA^{A608E} mutant (Fig. 9J-L). This bears from the fact that genes down-regulated in the RpoD^{L261Q} mutant are also down-regulated in the FusA^{A608E} mutant, thus leading to more extreme down-regulation in the FusA^{A608E}-RpoD^{L261Q} mutant (Fig. S20C).

Unfortunately we do not have information of this sort for the FusA^{A608E}-TopA^{S180L} mutant since we did not have the corresponding second site single mutant. However, it is possible that the interaction between the mutation in fusA and the mutation in *topA* must be extreme since we were unable to construct the *topA* single mutant.

Thus the mutation in a translation elongation factor has a large effect on the transcriptional state of the cell, beyond that indicated by threshold-dependent calls of differential expression, presumably through feedback from levels of partially folded proteins. The second-site mutations display epistasis with the FusA^{A608E} mutation, as manifested in their transcriptomes.

Genes with known roles to play in aminoglycoside resistance are mis-regulated in the mutants.

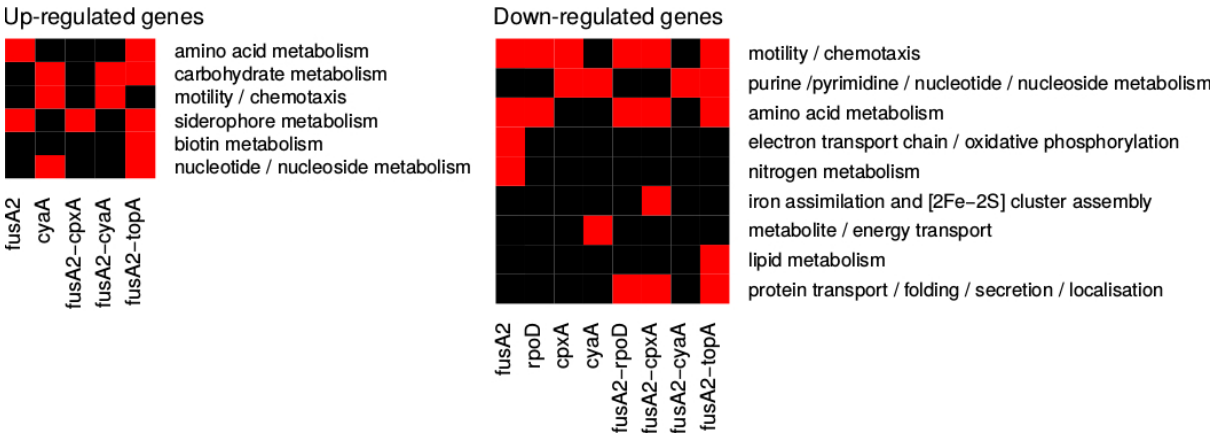

Figure 10: ***Significantly enriched groups of genes among differentially expressed genes in mutants.*** *Heatmap showing which gene ontology terms were enriched among the up and down-regulated genes in the mutants. Many gene ontology terms have been combined to give this simplified picture. For the entire set of terms and their P values refer to Fig. S21.*

Are the mechanisms of kanamycin resistance different or common across our set of mutants? To understand this, we looked at the kinds of genes differentially expressed in these mutants using gene ontology (GO) or known transcription factor-target interactions to guide us.

Common trends in terms of shared gene functions are outlined in (Fig. 10) and a more detailed list is provided in Fig. S21. In general, we found a lot of metabolism related genes mis-regulated in the mutants. Mis-regulated genes with known roles in aminoglycoside resistance include genes involved in oxidative phosphorylation, protein folding and motility.

Genes involved in oxidative phosphorylation are down-regulated in the FusA^{A6o8E} mutant. Oxidative phosphorylation produces reactive oxygen species (ROS), as a by-product, which is thought to be involved in antibiotic mediated killing (Kohanski et al., 2007). A functional proton motive force generated by oxidative phosphorylation is required for aminoglycoside uptake (Taber et al., 1987). Furthermore, the components of the electron transport chain (ETC) tend to be Fe-S proteins and are membrane associated. Mistranslation of membrane associated proteins induced by aminoglycosides, and hence their misfolding could affect the integrity of the cell membrane and result in hydroxyl radical mediated cell death (Kohanski et al., 2008). Misfolded versions of these proteins could also release Fenton reactive Fe^{2+}, which in turn could again result in hydroxyl radical generation (Kohanski et al., 2007). Thus, there are many ways in which down-regulating genes involved in oxidative phosphorylation, as in the FusA^{A6o8E} mutant, can alleviate the lethal effects of kanamycin.

Apart from these genes, genes associated with enterobactin biosynthesis or iron homeostasis are known to affect intracellular ROS levels (Méhi et al., 2014). It is possible that the up-regulation of these genes in the FusA^{A6o8E}, FusA^{A6o8E}-CpxA^{F218Y} and FusA^{A6o8E}-TopA^{S18oL} mutants could reduce the production of ROS in the cells via sequestration of free Fe^{2+} and hence contribute to resistance.

The downregulation of oxidative phosphorylation and the up-regulation of siderophore metabolism genes are in line with the hypothesis of oxidative damage mediated cell death in

the presence of antibiotics. While this theory is fiercely disputed, it is possible that ROS aggravate the effect of antibiotics, if not dominate it. For example, Ling et al., show that aminoglycoside induced protein aggregation is prevented by hydrogen peroxide quenchers (Ling et al., 2012). Dealing with ROS might result just in that extra protection that cells need in the presence of aminoglycosides.

ROS is a double edged sword. While it can damage cellular macromolecules and confer stress, the outcome of this stress could also result in an increase in mutagenesis (Kohanski, DePristo & Collins, 2010). Thus if these mutants do indeed reduce oxidative stress, it is quite possible that they will slow down further adaptation to kanamycin by reducing the occurrence of resistance conferring mutations. This however remains to be tested.

We see a strong and consistent down-regulation of motility associated genes, in all except the *cyaA* mutants. Using a transposon mutagenesis screen Shan et al., show that the loss of these genes results in decreased persister formation in aminoglycosides (Shan et al., 2015), and thus their down-regulation in the mutants is contrary to our expectation. However these genes are up-regulated in the CyaA^{N600Y} and FusA^{A608E}-CyaA^{N600Y} mutants and there they could contribute to resistance. Notably, motility genes are not found in the list of knockouts sensitive to aminoglycosides provided by Tamae et al. (Tamae et al., 2008), or in the list of loci that significantly affect susceptibility to aminoglycosides in the transposon insertion screen performed by Girgis et al (Girgis, Hottes & Tavazoie, 2009).

Motility genes have also been implicated in resistance to β-lactams, a completely different group of antibiotics, where the inactivation of these genes was shown to result in increased resistance (Girgis, Hottes & Tavazoie, 2009). Both aminoglycosides and β-lactams affect the cell surface integrity. Aminoglycosides can damage the cell by incorporation of misfolded proteins in the cell membrane and periplasmic space (Davis, Chen & Tai, 1986), and β-lactams damage the cell wall by inhibiting peptidoglycan biosynthesis (Waxman & Strominger, 1983). It is tempting to think that the flagellar complex, that is associated with the cell surface, and transverses the cell membrane as well as the cell wall, has a role to play in resistance to these two groups of antibiotics. The mechanism, however, remains to be understood.

Resistance to aminoglycosides can be provided by genes involved in protein transport/ folding/ secretion as these could help refold misfolded proteins (Goltermann, Good & Bentin, 2013). However, we see a down-regulation of these genes in the FusA^{A608E}-RpoD^{L261Q}, FusA^{A608E}-CpxA^{F218Y} and FusA^{A608E}-TopA^{S180L} mutants, and this is contrary to our expectation.

We also looked at which transcription factors regulate the genes differentially expressed in the mutants (Fig. S22). Some of these trends will mirror the GO trends that we report above. Such mirrored trends include the presence of Fur (ferric uptake regulator protein) and FecI (Sigma19, controls genes involved in ferric uptake) targets among the up-regulated genes in the FusA^{A608E}, FusA^{A608E}-CpxA^{F218Y} and FusA^{A608E}-TopA^{S180L} mutants and FlhDC /Sigma28 (motility associated sigma factor) targets among the down-regulated genes in all except the *cyaA* mutants. We also find that a large number of up-regulated genes tend to be CRP targets

and fewer so among the down-regulated genes. Again the striking similarity between the CpxA^{F218Y} and CyaA^{N600Y} single mutants is seen from this analysis. It is interesting that the EF-G mutant has a similar effect on the mutations in *cpxA* and *cyaA*. These similarities among mutants may indicate similar underlying mechanisms of resistance, a fact that is reflected in the presence of similar gene ontology terms among the mis-regulated genes across some of the mutants.

Conclusions

We saw that mutations that modify global transcriptional regulatory networks increase the resistance of the kanamycin conferring mutation in the translational elongation factor EF-G. These "second-site" mutations resulted in large changes in gene expression and displayed epistatic interactions with the mutation in EF-G, which itself drove expression changes of many genes. We show that these second site mutations reduce the activities of CyaA (adenylate cyclase) and possibly TopA (Topoisomerase I), and increase the activity of CpxA. Further evolution of an EF-G mutant in higher concentration of kanamycin suggested CpxA as the next target for an increase in resistance, with many high frequency mutations located in the helix-I domain of this protein. Although the activity of the mutated adenylate cyclase is reduced, many CRP targets are unexpectedly up-regulated and this contradictory behaviour needs further investigation. We suggest that FusA^{A608E}-TopA^{S180L} results in a reduction in the function of Topoisomerase I, while emphasising certain contradictions in the data used in these analyses. Many genes with known roles in aminoglycoside resistance, for example genes involved in oxidative phosphorylation and enterobactin metabolism, were mis-regulated in these mutants thus pointing to possible mechanisms of resistance.

Accession Numbers

RNA-seq data can be found on the NCBI Gene Expression Omnibus database (Edgar, Domrachev & Lash, 2002; Barrett et al., 2013) with the GEO Series accession number number GSE82343 (http://www.ncbi.nlm.nih.gov/geo/query/acc.cgi?acc=GSE82343). Genomic deep-sequencing data for the 15-kan evolution experiment can be accessed from the NCBI Sequence Read Archive (accession number: SRP076371).

Funding

This work was supported by the National Centre for Biological Sciences core funding. Funding to pay the Open Access publication charges for this article was provided by the National Centre for Biological Sciences, Tata Institute of Fundamental Research. ASNS is supported by a Ramanujan Fellowship (SR/S2/RJN-49/2010) from the Department of Science and Technology, India. AM is supported by an NCBS-TIFR studentship.

Acknowledgements

We thank Parul Singh for providing *E.coli* MG1655 Δ*cyaA* and Δ*crp* strains and for sharing the transcriptome data of these strains. Next-generation sequencing services were provided by C-CAMP and Genotypic, India.

References

Alexa A., Rahnenfuhrer J. 2010. *topGO: topGO: Enrichment analysis for Gene Ontology*.

Andersson DI. 2006. The biological cost of mutational antibiotic resistance: any practical conclusions? *Current Opinion in Microbiology* 9:461–465. DOI: 10.1016/j.mib.2006.07.002.

Andersson DI., Hughes D. 2010. Antibiotic resistance and its cost: is it possible to reverse resistance? *Nature Reviews. Microbiology* 8:260–271. DOI: 10.1038/nrmicro2319.

Andersson DI., Levin BR. 1999. The biological cost of antibiotic resistance. *Current Opinion in Microbiology* 2:489–493.

Balke VL., Gralla JD. 1987. Changes in the linking number of supercoiled DNA accompany growth transitions in Escherichia coli. *Journal of Bacteriology* 169:4499–4506.

Barrett T., Wilhite SE., Ledoux P., Evangelista C., Kim IF., Tomashevsky M., Marshall KA., Phillippy KH., Sherman PM., Holko M., Yefanov A., Lee H., Zhang N., Robertson CL., Serova N., Davis S., Soboleva A. 2013. NCBI GEO: archive for functional genomics data sets--update. *Nucleic Acids Research* 41:D991-995. DOI: 10.1093/nar/gks1193.

Becker B., Cooper MA. 2013. Aminoglycoside antibiotics in the 21st century. *ACS chemical biology* 8:105–115. DOI: 10.1021/cb3005116.

Bellon S., Parsons JD., Wei Y., Hayakawa K., Swenson LL., Charifson PS., Lippke JA., Aldape R., Gross CH. 2004. Crystal structures of Escherichia coli topoisomerase IV ParE subunit (24 and 43 kilodaltons): a single residue dictates differences in novobiocin potency against topoisomerase IV and DNA gyrase. *Antimicrobial Agents and Chemotherapy* 48:1856–1864.

Björkman J., Andersson DI. 2000. The cost of antibiotic resistance from a bacterial perspective. *Drug Resistance Updates: Reviews and Commentaries in Antimicrobial and Anticancer Chemotherapy* 3:237–245. DOI: 10.1054/drup.2000.0147.

Botsford JL., Harman JG. 1992. Cyclic AMP in prokaryotes. *Microbiological Reviews* 56:100–122.

Broccoli S., Rallu F., Sanscartier P., Cerritelli SM., Crouch RJ., Drolet M. 2004. Effects of RNA polymerase modifications on transcription-induced negative supercoiling and associated R-loop formation. *Molecular Microbiology* 52:1769–1779. DOI: 10.1111/j.1365-2958.2004.04092.x.

Bryan LE., Kwan S. 1983. Roles of ribosomal binding, membrane potential, and electron transport in bacterial uptake of streptomycin and gentamicin. *Antimicrobial Agents and Chemotherapy* 23:835–845.

Cheung KJ., Badarinarayana V., Selinger DW., Janse D., Church GM. 2003. A microarray-based antibiotic screen identifies a regulatory role for supercoiling in the osmotic stress response of Escherichia coli. *Genome Research* 13:206–215. DOI: 10.1101/gr.401003.

Corbalan N., Runti G., Adler C., Covaceuszach S., Ford RC., Lamba D., Beis K., Scocchi M., Vincent PA. 2013. Functional and structural study of the dimeric inner membrane protein SbmA. *Journal of Bacteriology* 195:5352–5361. DOI: 10.1128/JB.00824-13.

Crisona NJ., Strick TR., Bensimon D., Croquette V., Cozzarelli NR. 2000. Preferential relaxation of positively supercoiled DNA by E. coli topoisomerase IV in single-molecule and ensemble measurements. *Genes & Development* 14:2881–2892.

Davies J. 1996. Origins and evolution of antibiotic resistance. *Microbiología (Madrid, Spain)* 12:9–16.

Davis BD. 1987. Mechanism of bactericidal action of aminoglycosides. *Microbiological Reviews* 51:341–350.

Davis BD., Chen LL., Tai PC. 1986. Misread protein creates membrane channels: an essential step in the bactericidal action of aminoglycosides. *Proceedings of the National Academy of Sciences of the United States of America* 83:6164–6168.

Edgar R., Domrachev M., Lash AE. 2002. Gene Expression Omnibus: NCBI gene expression and hybridization array data repository. *Nucleic Acids Research* 30:207–210.

Feklístov A., Sharon BD., Darst SA., Gross CA. 2014. Bacterial sigma factors: a historical, structural, and genomic perspective. *Annual Review of Microbiology* 68:357–376. DOI: 10.1146/annurev-micro-092412-155737.

Feldman MB., Terry DS., Altman RB., Blanchard SC. 2010. Aminoglycoside activity observed on single pre-translocation ribosome complexes. *Nature Chemical Biology* 6:54–62. DOI: 10.1038/nchembio.274.

Fleischer R., Heermann R., Jung K., Hunke S. 2007. Purification, reconstitution, and characterization of the CpxRAP envelope stress system of Escherichia coli. *The Journal of Biological Chemistry* 282:8583–8593. DOI: 10.1074/jbc.M605785200.

Fournier B., Zhao X., Lu T., Drlica K., Hooper DC. 2000. Selective targeting of topoisomerase IV and DNA gyrase in Staphylococcus aureus: different patterns of

quinolone-induced inhibition of DNA synthesis. *Antimicrobial Agents and Chemotherapy* 44:2160–2165.

Gama-Castro S., Salgado H., Santos-Zavaleta A., Ledezma-Tejeida D., Muñiz-Rascado L., García-Sotelo JS., Alquicira-Hernández K., Martínez-Flores I., Pannier L., Castro-Mondragón JA., Medina-Rivera A., Solano-Lira H., Bonavides-Martínez C., Pérez-Rueda E., Alquicira-Hernández S., Porrón-Sotelo L., López-Fuentes A., Hernández-Koutoucheva A., Del Moral-Chávez V., Rinaldi F., Collado-Vides J. 2016. RegulonDB version 9.0: high-level integration of gene regulation, coexpression, motif clustering and beyond. *Nucleic Acids Research* 44:D133-143. DOI: 10.1093/nar/gkv1156.

Gene Ontology Consortium 2015. Gene Ontology Consortium: going forward. *Nucleic Acids Research* 43:D1049-1056. DOI: 10.1093/nar/gku1179.

Girgis HS., Hottes AK., Tavazoie S. 2009. Genetic architecture of intrinsic antibiotic susceptibility. *PloS One* 4:e5629. DOI: 10.1371/journal.pone.0005629.

Goltermann L., Good L., Bentin T. 2013. Chaperonins fight aminoglycoside-induced protein misfolding and promote short-term tolerance in Escherichia coli. *The Journal of Biological Chemistry* 288:10483–10489. DOI: 10.1074/jbc.M112.420380.

Gowrishankar J., Harinarayanan R. 2004. Why is transcription coupled to translation in bacteria? *Molecular Microbiology* 54:598–603. DOI: 10.1111/j.1365-2958.2004.04289.x.

Gowrishankar J., Leela JK., Anupama K. 2013. R-loops in bacterial transcription: their causes and consequences. *Transcription* 4:153–157.

Gubaev A., Klostermeier D. 2014. The mechanism of negative DNA supercoiling: a cascade of DNA-induced conformational changes prepares gyrase for strand passage. *DNA repair* 16:23–34. DOI: 10.1016/j.dnarep.2014.01.011.

Hardy CD., Cozzarelli NR. 2003. Alteration of Escherichia coli topoisomerase IV to novobiocin resistance. *Antimicrobial Agents and Chemotherapy* 47:941–947.

Hsieh LS., Burger RM., Drlica K. 1991. Bacterial DNA supercoiling and [ATP]/[ADP]. Changes associated with a transition to anaerobic growth. *Journal of Molecular Biology* 219:443–450.

Hunke S., Keller R., Müller VS. 2012. Signal integration by the Cpx-envelope stress system. *FEMS microbiology letters* 326:12–22. DOI: 10.1111/j.1574-6968.2011.02436.x.

Isaac DD., Pinkner JS., Hultgren SJ., Silhavy TJ. 2005. The extracytoplasmic adaptor protein CpxP is degraded with substrate by DegP. *Proceedings of the National*

Academy of Sciences of the United States of America 102:17775–17779. DOI: 10.1073/pnas.0508936102.

Karp PD., Weaver D., Paley S., Fulcher C., Kubo A., Kothari A., Krummenacker M., Subhraveti P., Weerasinghe D., Gama-Castro S., Huerta AM., Muñiz-Rascado L., Bonavides-Martinez C., Weiss V., Peralta-Gil M., Santos-Zavaleta A., Schröder I., Mackie A., Gunsalus R., Collado-Vides J., Keseler IM., Paulsen I. 2014. The EcoCyc Database. *EcoSal Plus* 6. DOI: 10.1128/ecosalplus.ESP-0009-2013.

Kato J., Nishimura Y., Imamura R., Niki H., Hiraga S., Suzuki H. 1990. New topoisomerase essential for chromosome segregation in E. coli. *Cell* 63:393–404.

Kern WV., Oethinger M., Jellen-Ritter AS., Levy SB. 2000. Non-target gene mutations in the development of fluoroquinolone resistance in Escherichia coli. *Antimicrobial Agents and Chemotherapy* 44:814–820.

Koboldt DC., Zhang Q., Larson DE., Shen D., McLellan MD., Lin L., Miller CA., Mardis ER., Ding L., Wilson RK. 2012. VarScan 2: somatic mutation and copy number alteration discovery in cancer by exome sequencing. *Genome Research* 22:568–576. DOI: 10.1101/gr.129684.111.

Kohanski MA., Dwyer DJ., Hayete B., Lawrence CA., Collins JJ. 2007. A common mechanism of cellular death induced by bactericidal antibiotics. *Cell* 130:797–810. DOI: 10.1016/j.cell.2007.06.049.

Kohanski MA., Dwyer DJ., Wierzbowski J., Cottarel G., Collins JJ. 2008. Mistranslation of membrane proteins and two-component system activation trigger antibiotic-mediated cell death. *Cell* 135:679–690. DOI: 10.1016/j.cell.2008.09.038.

Kohanski MA., DePristo MA., Collins JJ. 2010. Sublethal antibiotic treatment leads to multidrug resistance via radical-induced mutagenesis. *Molecular Cell* 37:311–320. DOI: 10.1016/j.molcel.2010.01.003.

Kotra LP., Haddad J., Mobashery S. 2000. Aminoglycosides: perspectives on mechanisms of action and resistance and strategies to counter resistance. *Antimicrobial Agents and Chemotherapy* 44:3249–3256.

Laviña M., Pugsley AP., Moreno F. 1986. Identification, mapping, cloning and characterization of a gene (sbmA) required for microcin B17 action on Escherichia coli K12. *Journal of General Microbiology* 132:1685–1693. DOI: 10.1099/00221287-132-6-1685.

Lázár V., Pal Singh G., Spohn R., Nagy I., Horváth B., Hrtyan M., Busa-Fekete R., Bogos B., Méhi O., Csörgő B., Pósfai G., Fekete G., Szappanos B., Kégl B., Papp B., Pál C. 2013.

Bacterial evolution of antibiotic hypersensitivity. *Molecular Systems Biology* 9:700. DOI: 10.1038/msb.2013.57.

Leibman M., Hochschild A. 2007. A sigma-core interaction of the RNA polymerase holoenzyme that enhances promoter escape. *The EMBO journal* 26:1579–1590. DOI: 10.1038/sj.emboj.7601612.

Lenski RE. 1998. Bacterial evolution and the cost of antibiotic resistance. *International Microbiology: The Official Journal of the Spanish Society for Microbiology* 1:265–270.

Levy SB., Marshall B. 2004. Antibacterial resistance worldwide: causes, challenges and responses. *Nature Medicine* 10:S122-129. DOI: 10.1038/nm1145.

Li H., Handsaker B., Wysoker A., Fennell T., Ruan J., Homer N., Marth G., Abecasis G., Durbin R., 1000 Genome Project Data Processing Subgroup 2009. The Sequence Alignment/Map format and SAMtools. *Bioinformatics (Oxford, England)* 25:2078–2079. DOI: 10.1093/bioinformatics/btp352.

Li H., Durbin R. 2010. Fast and accurate long-read alignment with Burrows-Wheeler transform. *Bioinformatics (Oxford, England)* 26:589–595. DOI: 10.1093/bioinformatics/btp698.

Ling J., Cho C., Guo L-T., Aerni HR., Rinehart J., Söll D. 2012. Protein aggregation caused by aminoglycoside action is prevented by a hydrogen peroxide scavenger. *Molecular Cell* 48:713–722. DOI: 10.1016/j.molcel.2012.10.001.

López V., Martínez-Robles M-L., Hernández P., Krimer DB., Schvartzman JB. 2012. Topo IV is the topoisomerase that knots and unknots sister duplexes during DNA replication. *Nucleic Acids Research* 40:3563–3573. DOI: 10.1093/nar/gkr1237.

Mahoney TF., Silhavy TJ. 2013. The Cpx stress response confers resistance to some, but not all, bactericidal antibiotics. *Journal of Bacteriology* 195:1869–1874. DOI: 10.1128/JB.02197-12.

Manoil C. 2013. Clarifying the role of two-component regulation in antibiotic killing. *Journal of Bacteriology* 195:1857–1858. DOI: 10.1128/JB.00190-13.

Martin M. 2011. Cutadapt removes adapter sequences from high-throughput sequencing reads. *EMBnet.journal* 17:10. DOI: 10.14806/ej.17.1.200.

Massé E., Drolet M. 1999. Escherichia coli DNA topoisomerase I inhibits R-loop formation by relaxing transcription-induced negative supercoiling. *The Journal of Biological Chemistry* 274:16659–16664.

McClellan JA., Boublíková P., Palecek E., Lilley DM. 1990. Superhelical torsion in cellular DNA responds directly to environmental and genetic factors. *Proceedings of the National Academy of Sciences of the United States of America* 87:8373–8377.

McDonough KA., Rodriguez A. 2012. The myriad roles of cyclic AMP in microbial pathogens: from signal to sword. *Nature Reviews. Microbiology* 10:27–38. DOI: 10.1038/nrmicro2688.

Méhi O., Bogos B., Csörgő B., Pál F., Nyerges A., Papp B., Pál C. 2014. Perturbation of iron homeostasis promotes the evolution of antibiotic resistance. *Molecular Biology and Evolution* 31:2793–2804. DOI: 10.1093/molbev/msu223.

Menzel R., Gellert M. 1987. Fusions of the Escherichia coli gyrA and gyrB control regions to the galactokinase gene are inducible by coumermycin treatment. *Journal of Bacteriology* 169:1272–1278.

Mogre A., Sengupta T., Veetil RT., Ravi P., Seshasayee ASN. 2014. Genomic analysis reveals distinct concentration-dependent evolutionary trajectories for antibiotic resistance in Escherichia coli. *DNA research: an international journal for rapid publication of reports on genes and genomes* 21:711–726. DOI: 10.1093/dnares/dsu032.

Paulsen VS., Mardirossian M., Blencke H-M., Benincasa M., Runti G., Nepa M., Haug T., Stensvåg K., Scocchi M. 2016. Inner membrane proteins YgdD and SbmA are required for the complete susceptibility of E. coli to the proline-rich antimicrobial peptide arasin 1(1-25). *Microbiology (Reading, England)*. DOI: 10.1099/mic.0.000249.

Peter BJ., Arsuaga J., Breier AM., Khodursky AB., Brown PO., Cozzarelli NR. 2004. Genomic transcriptional response to loss of chromosomal supercoiling in Escherichia coli. *Genome Biology* 5:R87. DOI: 10.1186/gb-2004-5-11-r87.

Pogliano J., Lynch AS., Belin D., Lin EC., Beckwith J. 1997. Regulation of Escherichia coli cell envelope proteins involved in protein folding and degradation by the Cpx two-component system. *Genes & Development* 11:1169–1182.

Pruss GJ., Drlica K. 1989. DNA supercoiling and prokaryotic transcription. *Cell* 56:521–523.

R Core Team 2016. *R: A Language and Environment for Statistical Computing*. Vienna, Austria: R Foundation for Statistical Computing.

Raivio TL., Laird MW., Joly JC., Silhavy TJ. 2000. Tethering of CpxP to the inner membrane prevents spheroplast induction of the cpx envelope stress response. *Molecular Microbiology* 37:1186–1197.

Raivio TL., Popkin DL., Silhavy TJ. 1999. The Cpx envelope stress response is controlled by amplification and feedback inhibition. *Journal of Bacteriology* 181:5263–5272.

Raivio TL., Silhavy TJ. 1997. Transduction of envelope stress in Escherichia coli by the Cpx two-component system. *Journal of Bacteriology* 179:7724–7733.

Robinson MD., McCarthy DJ., Smyth GK. 2010. edgeR: a Bioconductor package for differential expression analysis of digital gene expression data. *Bioinformatics (Oxford, England)* 26:139–140. DOI: 10.1093/bioinformatics/btp616.

Rui S., Tse-Dinh Y-C. 2003. Topoisomerase function during bacterial responses to environmental challenge. *Frontiers in Bioscience: A Journal and Virtual Library* 8:d256-263.

Runti G., Lopez Ruiz M del C., Stoilova T., Hussain R., Jennions M., Choudhury HG., Benincasa M., Gennaro R., Beis K., Scocchi M. 2013. Functional characterization of SbmA, a bacterial inner membrane transporter required for importing the antimicrobial peptide Bac7(1-35). *Journal of Bacteriology* 195:5343–5351. DOI: 10.1128/JB.00818-13.

Saier MH., Yen MR., Noto K., Tamang DG., Elkan C. 2009. The Transporter Classification Database: recent advances. *Nucleic Acids Research* 37:D274-278. DOI: 10.1093/nar/gkn862.

Salomón RA., Farías RN. 1995. The peptide antibiotic microcin 25 is imported through the TonB pathway and the SbmA protein. *Journal of Bacteriology* 177:3323–3325.

Shan Y., Lazinski D., Rowe S., Camilli A., Lewis K. 2015. Genetic basis of persister tolerance to aminoglycosides in Escherichia coli. *mBio* 6. DOI: 10.1128/mBio.00078-15.

Snoep JL., van der Weijden CC., Andersen HW., Westerhoff HV., Jensen PR. 2002. DNA supercoiling in Escherichia coli is under tight and subtle homeostatic control, involving gene-expression and metabolic regulation of both topoisomerase I and DNA gyrase. *European journal of biochemistry / FEBS* 269:1662–1669.

Strozen TG., Langen GR., Howard SP. 2005. Adenylate cyclase mutations rescue the degP temperature-sensitive phenotype and induce the sigma E and Cpx extracytoplasmic stress regulons in Escherichia coli. *Journal of Bacteriology* 187:6309–6316. DOI: 10.1128/JB.187.18.6309-6316.2005.

Stupina VA., Wang JC. 2005. Viability of Escherichia coli topA mutants lacking DNA topoisomerase I. *The Journal of Biological Chemistry* 280:355–360. DOI: 10.1074/jbc.M411924200.

Taber HW., Mueller JP., Miller PF., Arrow AS. 1987. Bacterial uptake of aminoglycoside antibiotics. *Microbiological Reviews* 51:439–457.

Tamae C., Liu A., Kim K., Sitz D., Hong J., Becket E., Bui A., Solaimani P., Tran KP., Yang H., Miller JH. 2008. Determination of antibiotic hypersensitivity among 4,000 single-gene-knockout mutants of Escherichia coli. *Journal of Bacteriology* 190:5981–5988. DOI: 10.1128/JB.01982-07.

Thanbichler M., Shapiro L. 2006. Chromosome organization and segregation in bacteria. *Journal of Structural Biology* 156:292–303. DOI: 10.1016/j.jsb.2006.05.007.

Thanbichler M., Wang SC., Shapiro L. 2005. The bacterial nucleoid: a highly organized and dynamic structure. *Journal of Cellular Biochemistry* 96:506–521. DOI: 10.1002/jcb.20519.

Thomason LC., Costantino N., Court DL. 2007. E. coli genome manipulation by P1 transduction. *Current Protocols in Molecular Biology / Edited by Frederick M. Ausubel ... [et Al.]* Chapter 1:Unit 1.17. DOI: 10.1002/0471142727.mb0117s79.

Toro E., Shapiro L. 2010. Bacterial chromosome organization and segregation. *Cold Spring Harbor Perspectives in Biology* 2:a000349. DOI: 10.1101/cshperspect.a000349.

Travers A., Muskhelishvili G. 2005. DNA supercoiling - a global transcriptional regulator for enterobacterial growth? *Nature Reviews. Microbiology* 3:157–169. DOI: 10.1038/nrmicro1088.

Tse-Dinh YC., Beran RK. 1988. Multiple promoters for transcription of the Escherichia coli DNA topoisomerase I gene and their regulation by DNA supercoiling. *Journal of Molecular Biology* 202:735–742.

Usongo V., Nolent F., Sanscartier P., Tanguay C., Broccoli S., Baaklini I., Drlica K., Drolet M. 2008. Depletion of RNase HI activity in Escherichia coli lacking DNA topoisomerase I leads to defects in DNA supercoiling and segregation. *Molecular Microbiology* 69:968–981. DOI: 10.1111/j.1365-2958.2008.06334.x.

Vogt SL., Raivio TL. 2012. Just scratching the surface: an expanding view of the Cpx envelope stress response. *FEMS microbiology letters* 326:2–11. DOI: 10.1111/j.1574-6968.2011.02406.x.

Waxman DJ., Strominger JL. 1983. Penicillin-binding proteins and the mechanism of action of beta-lactam antibiotics. *Annual Review of Biochemistry* 52:825–869. DOI: 10.1146/annurev.bi.52.070183.004141.

Woldringh CL. 2002. The role of co-transcriptional translation and protein translocation (transertion) in bacterial chromosome segregation. *Molecular Microbiology* 45:17–29.

Yorgey P., Lee J., Kördel J., Vivas E., Warner P., Jebaratnam D., Kolter R. 1994. Posttranslational modifications in microcin B17 define an additional class of DNA gyrase inhibitor. *Proceedings of the National Academy of Sciences of the United States of America* 91:4519–4523.

Zechiedrich EL., Khodursky AB., Cozzarelli NR. 1997. Topoisomerase IV, not gyrase, decatenates products of site-specific recombination in Escherichia coli. *Genes & Development* 11:2580–2592.

Zheng D., Constantinidou C., Hobman JL., Minchin SD. 2004. Identification of the CRP regulon using in vitro and in vivo transcriptional profiling. *Nucleic Acids Research* 32:5874–5893. DOI: 10.1093/nar/gkh908.